Chapter 4: Comprehensive agent-based modeling at the pathogen-host-environment interface for simulating the spread of emerging diseases

Chapter 4.1: CalCWD: An agent-based model for simulating chronic wasting disease dynamics in mule deer in California

Abstract

Chronic Wasting Disease (CWD) is a fatal neurodegenerative prion disease affecting cervids. Initially detected in 1967 in Colorado, CWD has since spread extensively across North America and beyond, posing significant threats to wildlife populations and socio-economic structures. This study develops an agent-based model to simulate the spatiotemporal dynamics of CWD in mule deer (*Odocoileus hemionus*) population in California, focusing on the interplay between ecological and epidemiological factors unique to the region, such as host migratory behavior and environmental challenges like droughts and wildfires. The entities within the model include deer individuals, infectious carcasses, and grid cells, each characterized by multiple state variables related to the environment, demographics, behavior, and disease status. These entities evolve spatiotemporally and interact with each other through processes. These processes are divided into two main modules: an ecological module and an epidemiological module. The ecological module simulates mule deer population dynamics influenced by natural phenomena such as fires and droughts, as well as anthropogenic factors like hunting pressure. The model accounts for a range of processes, including aging, natural and hunting mortality, fawning, seasonal group dynamics, yearling dispersal, and seasonal migrations. The epidemiological module simulates the spread of CWD, which interacts with and impacts the deer population. In this way, the spatiotemporal dynamics of the disease emerge from the model, influenced by and in turn influencing the mule deer population dynamics. The epidemiological module considers transmission through direct contact, environmental prion presence, and infectious carcasses. The model is parametrized through stochastic elements to reflect the probabilistic nature of pathogen transmission and demographic events. Evaluation of the model's ecological module over a 50-year simulation shows a slight decline in mule deer populations, consistent with historical data. The epidemiological module, tested over seven years of pathogen spread, accurately replicates known CWD patterns,

including higher prevalence in bucks and a spread rate of 7.1 km/year matching empirical observations. This model provides a reliable framework for understanding CWD dynamics in California, offering insights into the potential impacts of environmental factors and pathogen spread. This model could serve as a valuable tool for wildlife management and the design of disease monitoring and control strategies. By adjusting input parameters, the model can be adapted for use in other regions and for other cervid species, enhancing its applicability for broader wildlife disease management efforts.

Keywords: Agent-based model, California, chronic wasting disease, disease spread, ecological modeling, epidemiological modeling, mule deer, simulation, wildlife epidemiology

1. Introduction

Chronic Wasting Disease (CWD) is a Transmissible Spongiform Encephalopathy (TSE) that affects members of the Cervidae family. Like other TSEs, such as sheep scrapie, bovine spongiform encephalopathy (BSE or "mad cow" disease), or Creutzfeldt-Jakob disease (CJD) in humans, CWD is caused by a prion, an abnormally folded and proteinase-resistant isoform (PrP^{res}) of a prion protein, the cellular glycoprotein (PrP^{c}), which is naturally found in the brain (Johnson 2005). The triggering prion, PrP^{CWD} in the case of CWD, is capable of inducing abnormal folding in other proteins, leading to a neurodegenerative disease and ultimately to death (Johnson *et al.* 2011; Williams 2005). Given its lethal nature, the high prevalences detected in both domestic and wild individuals (Mysterud & Edmunds 2019) pose a significant socio-economic threat, as well as a threat to the conservation of host species, capable of causing population declines (DeVivo *et al.* 2017; Edmunds *et al.* 2016).

The initial case of CWD was identified in 1967 in captive mule deer (*Odocoileus hemionus*) in the state of Colorado, USA, although it was not classified as a TSE until 1980 (Williams & Young 1980). Subsequently, it was also detected in white-tailed deer (*Odocoileus virginianus*) and elk (*Cervus canadensis*) in Colorado, Wyoming, and Alberta (Canada). The disease was primarily observed in captive individuals, but it also affected wild populations (Spraker *et al.* 1997). Until 2000, the disease had a limited distribution (Otero *et al.* 2021). However, since then, it has spread extensively across North America, currently affecting 34 states in the USA and 5 provinces in Canada (NWHC 2024), as well as other continents, with cases in captive cervids in South Korea and in wild cervids in Finland, Sweden, and Norway (Baeten *et al.* 2007; Benestad *et al.* 2016; Kim *et al.* 2005; NWHC 2024). This has expanded the list of naturally susceptible species to include moose (*Alces alces*), caribou (*Rangifer tarandus*), and red deer (*Cervus elaphus;* Escobar *et al.* 2020).

The most recent state to be added to the list is California, where two cases have been identified in different areas of the state (NWHC 2024). California presents a unique scenario for analyzing the potential spread of the CWD. Firstly, a portion of the mule deer population is migratory (Monteith *et al.* 2011), which represents a pathway for long-distance pathogen spread (Diefenbach *et al.* 2008; Farnsworth *et al.* 2006; Garlick *et al.* 2014). Secondly, California is prone to experiencing forest fires and multi-year droughts, with several implications for wildlife (Littell *et al.* 2016; Madadgar *et al.* 2020; Mount, Escriva-Bou & Sencan 2021). On the one hand, wildfires may result in the dispersal of mule deer individuals (van Mantgem, Keeley & Witter 2015), which could potentially increase the risk of pathogen expansion. On the other hand, droughts may affect host survival rates and aggregation, thereby influencing pathogen transmission (Jackson *et al.* 2021; Miller & Conner 2005; Schuyler, Dugger & Jackson 2018).

The low prevalence of the disease at the early stages of its emergence, the long infectious periods before clinical signs appear, the irregular distribution of the disease among sexes and age classes, and the unbalanced sampling derived from the use of samples from hunting, make disease spread monitoring challenging (Belsare *et al.* 2020a; Haley & Hoover 2015; Mysterud & Edmunds 2019). This results in a dearth of empirical data that would permit the analysis of the spatiotemporal dynamics of the disease from a top-down approach, the most common in CWD epidemiological studies, in which the potential of factors employed as proxies of processes to explain observed patterns is assessed (Winter & Escobar 2020). Agent-based models (ABMs) present an alternative to simulate disease dynamics in this type of scenario (Belsare & Stewart 2020). ABMs follow a bottom-up approach, wherein processes are parameterized at the individual or group level and scaled up to patterns at the population level (Grimm *et al.* 2005). This approach allows for simulating pathogen expansion at a regional scale in novel scenarios based on known processes at a local scale (Lane-deGraaf *et al.* 2013; McCallum 2016).

Our aim was to build an ABM capable of simulating the dynamics of CWD in natural populations of the state of California, considering both the specific climatic conditions and the demographic, social, and behavioral aspects of the mule deer population, which is the main natural host present in the region (Escobar *et al.* 2020). The model was developed in GAMA Platform (Taillandier *et al.* 2018). Model description following ODD protocol (Overview, Design Concepts and Details; Grimm *et al.* 2010; 2020) is shown below.

2. ODD Protocol

2.1. Purpose

The purpose of the model is to simulate the spatiotemporal dynamics of CWD in mule deer in the state of California. To achieve this, the model comprises two main modules:

1. The ecological module, which pertains to the host, and whose purpose is to simulate the mule deer population in California over time and space, considering its response to both natural phenomena, such as fires or droughts, and anthropogenic factors, such as hunting. This module is comprised of two submodules. The first submodule pertains to the environment, and encompasses data and processes such as habitat suitability, scavenging pressure, wildfires, and droughts. The second submodule pertains to the host and includes demographic, social, and behavioral information about mule deer, such as natality, mortality, migrations and grouping patterns.
2. The epidemiological module, which is related to the pathogen, and whose purpose is to examine the spread of CWD over time in the mule deer population. This module interacts with the ecological one. The evolution of the deer population affects the pathogen spread, which in turn affects the population by causing mortality.

2.2. Entities, state variables, and scales

The model comprises three agents as entities: deer, carcass, and grid cells. The discretization of the space into grid cell agents allows some processes to be programmed at the cell level, thereby reducing the computational cost and increasing the ability to apply a complex model to large scales.

Entity	State variable	Description
Deer	*cell*	id of the grid cell in which deer is located
	residence	id of the grid cell where deer resides
	sex	1 for male and 0 for female
	age	Age in days
	class	1 if fawn, 2 if yearling, 3 if adult, 4 if old
	fawning	1 if pregnant female, 0 otherwise
	mother	id of the mother
	group	id of the group to which it belongs
	solitary	1 if solitary, 0 otherwise
	migratory	1 if it belongs to a migratory population, 0 otherwise
	susceptible	1 if uninfected, 0 otherwise
	exposed	1 if infected but not infectious, 0 otherwise
	infected	1 if infected and infectious, 0 otherwise
	clinical	1 if infected with clinical signs, 0 otherwise
Carcass	*loc*	id of the grid cell in which the deer infectious carcass is located
	removal	Number of days the carcass remains in the environment
Grid cell	*N*	Mule deer abundance
	migra	Mule deer range: 1 if summer range, 2 winter range, 3 if year-round, -1 otherwise
	K	Number of mule deer that the grid cell can shelter
	weight	Cell resistance
	huntpressure	Proportion of the population annually harvested
	prevalence	CWD prevalence in the cell
	ncarcass	Number of deer infectious carcasses in the cell
	scavengers	1 to 5 depending on the number of present scavengers' species
	daysburnt	Days elapsed since the cell was burnt

Table 1. Entities and their states variables included in the simulation.

Each deer is defined by 14 state variables related to location, age, sex, fawning, grouping, migratory behavior, and CWD infection status. When an infected deer dies, it becomes a carcass agent, with the location and the days of persistence in the environment as state variables. Grid cells have 9 state variables related to habitat suitability, carrying capacity (*K*), deer range (year-round, winter, summer, or out of the range), deer abundance (*N*), infectious deer carcass abundance, CWD prevalence, scavenging pressure, hunting pressure and whether the cell has been damaged by fire. The entities included in the model and their state variables are shown in Table 1.

The spatial extent of the grid encompasses the California state, being each grid cell a 10 km x 10 km size square (100 km^2). The model has a daily time step, starting in the middle of the summer (day = 213; August 1st).

2.3. Process overview and scheduling

Processes referred to the deer agent in the model are related to: 1) mule deer population dynamics; and 2) CWD disease dynamics in the mule deer population. Population dynamics processes include aging, natural mortality, hunting mortality, fawning, seasonal group dynamics, yearling dispersal, and seasonal migrations. The CWD disease dynamics processes include pathogen transmission or exposition and CWD-induced mortality.

Processes related with the mule deer population dynamics are scheduled as follows (Ahlborn & White 2006; Mejia-Salazar *et al.* 2017; Monteith *et al.* 2011): On December 16th (day = 350) early gestation (EG) starts, and large mixed groups are formed. On April 1st (day = 91) late gestation (LG) period starts, during which males separate from females and young individuals. Departure from winter range areas to summer range (spring migration) begin in middle April (day = 105). Fawning (F) starts on May 16th (day = 136), resulting in the formation of the smallest groups of the year. Females go apart for giving birth, while fawns from

the previous year separate from their mothers' group and disperse. On August 1st (day = 213) pre-rut (PR) period begins, and males start joining females with fawns. Females without fawns remain in small groups. Hunting mortality occurs between August 14th (day = 226) and November 7th (day = 311). Fall migration commences in mid-October (day = 288). Rut (R) period begins on November 1st (day = 305). Aging and natural mortality occur every step. The day starts from 0 (1st January) after it reaches 365 (31st December).

With regard to the CWD processes scheduling, prion shedding commences 6 to 9 months (180 to 270 days) after infection (Plummer *et al.* 2017; Tamguney *et al.* 2009), thereby enabling direct transmission and environmental deposition. Clinical signs manifest approximately 490 days after infection (Johnson *et al.* 2011; Williams 2005). Death by disease takes place 14 to 120 days after the onset of clinical signs (Williams 2005). Following death, infected deer become a carcass agent, which remains infectious (Miller *et al.* 2004). The only process considered for the carcasses is their disappearance. The time carcasses remain in the environment depends on the season and scavenging pressure (Jennelle *et al.* 2009).

The processes referred to the grid cells are droughts, wildfires, and the diffusion of CWD across neighboring cells. Drought has a given probability of occurring at the start of the simulation and can last for a number of days derived from a uniform distribution between 365 and 1460 days (1 to 4 years; Miller *et al.* 2022). During the summer months, wildfires may occur in cells with a certain probability, affecting carrying capacity (Bristow *et al.* 2020; Sparks *et al.* 2018).

2.4. Design concepts

2.4.1. Basic principles

Density dependence in mule deer was assumed to be related with the carrying capacity in the winter range, which entails an effect on fawn survival in

winter but not on adult survival (Bergman *et al.* 2015). The buck:doe ratio was considered not to affect the birth rates since no severe decline in productivity was found as a response to the sex ratio (White *et al.* 2001). Predation, primarily by coyote (*Canis latrans*) and mountain lion (*Puma concolor*), could influence mortality rates in the overall population, particularly in fawns. However, several studies have shown changes in predator communities entailing compensatory effects, leading to the absence of changes in population trends (for further information, see Forrester & Wittmer 2013). Therefore, no changes in mule deer demography based on predator community composition were assumed in the model.

This model assumes that CWD can be transmitted through direct animal contact or through the environmental presence of the prion, either in the soil or in an infectious carcass (Miller, Hobbs & Tavener 2006). Furthermore, it assumes a CWD diffusion process from where the outbreak originates (Jennelle *et al.* 2014). Vertical transmission was omitted in the model since it is unusual (Miller & Williams 2003) and seems no to have an effect on the disease dynamics (Potapov *et al.* 2013). In addition to mortality due to CWD, the model assumes an increase in mortality of infected deer due to greater susceptibility to predation, vehicle kill, dehydration, or hypothermia during winter months (Miller *et al.* 2008; Otero *et al.* 2021).

Long-range movements may also play an important role in the spread of the pathogen to farer areas (Diefenbach *et al.* 2008; Garlick *et al.* 2014). Therefore, dispersal and migration were incorporated into the model. Mule deer populations in California can be resident or migratory (Ahlborn & White 2006). Resident populations were assumed to remain in the same cell throughout the year, while migratory populations were assumed to move entirely from summer to winter range cells in fall migration, returning to the cell where they were born in spring migration (van de Kerk *et al.* 2021). Dispersion is carried out by yearlings, mainly males but also females (Robinette 1966), Displacements can occur in any

direction within the range (Hamlin & Mackie 1989). Cells selected for migratory displacements were assumed to depend on habitat suitability, slope, and its traditional use as migratory corridors. Upon reaching the target cell, the probability of the deer remaining in that cell or moving on to another suitable cell is assumed to depend on the N and K values of the cell, leading to dispersion towards another cell when N approaches K.

The model assumes that drought leads to an increase in mortality and in the probability of wildfires (Jackson *et al.* 2021; Littell *et al.* 2016; Schuyler, Dugger & Jackson 2018). With regard to wildfires, it is assumed that when they occur, the environmental prion load of the cell is eliminated (Lee 2023). Moreover, it is postulated that wildfires have an effect on the cell's K, reducing it to a minimum during the first year after the fire and almost doubling during the second year, then stabilizing over the next three years (Bristow *et al.* 2020; Sparks *et al.* 2018).

2.4.2. Emergence

The CWD spread emerges from the model based on the mule deer population, grouping and movement patterns, and on transmission dynamics. Mule deer mortality is also influenced by population abundance and CWD prevalence rates, so mule deer population dynamics itself also emerges from the model.

2.4.3. Adaptation

The mule deer adapt their behavior based on N and K. When N approaches K, either due to an increase in population or a sharp reduction in K as a result of a wildfire, the mule deer disperse to other cells that have the capacity to accommodate them.

2.4.4. Sensing

The mule deer agents sense the state variables of the grid cell agents, which influence the probability of being hunted, the destination and movement cells for migratory and dispersal movements, and the probability of infection through environmental prion load or the presence of infectious carcasses. Conversely, grid cells also sense mule deer agents, as they sense the number of deer they contain and how many of them are infected, thus determining N, the prevalence of CWD, and the prion load. Moreover, they also sense the presence of infectious carcass agents. Finally, there is also sensing among the mule deer agents themselves, which determines group dynamics and transmission within them, and among the grid cell agents themselves, determining the spread of fires or the diffusion of the pathogen between cells.

2.4.5. Interaction

Deer agents can interact being able to entail pathogen transmission if one of them is infected and the other one is not. Deer agents can interact with infected deer carcasses agents being able to acquire the pathogen if they are not infected. Deer agents also interact with the grid cell agents, as the prion load of each cell is determined by infected deer that are or have been in it. This prion load can, in turn, lead to the infection. Additionally, grid cell agents interact with each other, as the CWD diffusion process considers new infection in a cell based on the prevalence of neighboring cells.

2.4.6. Stochasticity

Natality (i.e., the number of offspring per female and the occurrence of twins, as well as the sex of the offspring), mortality (both natural and hunting-related mortality), and dispersal, are based on probabilities that affect each individual, and therefore are stochastic processes. Hunting is also a stochastic

process since hunting pressure is defined by a Gamma distribution. These demographic processes condition mule deer abundance, influencing cell selection during migration and thus making this process also stochastic. Moreover, the day on which each individual migrates is also stochastic, conditioning the abundance on the target cell at the time of its arrival, and therefore influencing cell selection. Group dynamics is also a stochastic process in which size is provided as a range and the members are randomly selected based on the size and sex and age ratios for each season. All transmission processes and durations of each infection status are stochastic as they are based on probabilities and variable time intervals. Drought has a probability of occurring at the beginning of the simulation, and its duration is variable. Each cell has a certain probability of being burnt by a wildfire each summer.

2.4.7. Collectives

Deer agents are organized in social groups that fluctuate in size and sex and age ratios seasonally. The transmission processes of CWD differ within and outside of these groups.

2.5. Initialization

The initial sex and age ratios of the mule deer population are shown in Table 2. All deer are initially susceptible to infection. The outbreak initiates with the infection of an adult male, based on observed infection rates (Miller & Conner 2005; Osnas *et al.* 2009). The location and start date of the outbreak can be selected for each simulation. Mule deer demographic and epidemiological parameters employed for the simulation are described in Tables 3 and 4, respectively.

Table 2. Initial proportion of the population by sex and age based on Furnas *et al.* (2018); Rittenhouse, Mong and Hart (2015); Wood *et al.* (1989).

	Initial proportion of the population
Fawn male (0 - 1 year)	0.17
Fawn female (0 - 1 year)	0.17
Yearling male (1 - 2 years)	0.11
Yearling female (1 - 2 years)	0.14
Adult male (2 - 9 years)	0.09
Adult female (2 - 11 years)	0.25
Old male (9 - 12 years)	0.02
Old female (11 - 16 years)	0.05

The California Department of Fish and Wildlife (CDFW) provided the proportion of mule deer population for each cell (Munk and Heeren, unpublished data; see Figure 1). The initial value of mule deer abundance (N) is obtained by multiplying this proportion by the total mule deer population in the state of California, which value can be adjusted for better computational performance. The type of range for each cell (summer range, winter range, or year-round range) was also provided by the CDFW (see Figure 1).

The K was considered to be associated with the habitat suitability (Muñoz *et al.* 2015). Therefore, a habitat suitability (hs) value for each cell was calculated from land cover based on the Stanke *et al.* (2018) classification. Given the set of grid cells n, which comprises the overall state of California, the K of a given grid cell i was calculated by considering the maximum N of the set of cells n and the habitat suitability (hs) as follows:

$$K_i = hs_i \cdot \max\{N_n\} \quad (1)$$

Table 3. Mule deer demographic parameters employed for the modeling. PR is the pre-rut period, R is the rut period, EG is the early gestation period, LG is the late gestation period, and F is the fawning period.

Parameter	Description	Value	Source
preg	Proportion of females that get pregnant (yearling; adult; old)	0.6; 0.87; 0.8	Bender and Hoenes (2018); Monteith *et al.* (2014); Taylor (1996)
fawnsex	male:female sex ratio at birth	1:1	Taylor (1996)
twinp	Twin probability given pregnancy (yearling; adult; old)	0.07; 0.87; 0.29	Bender and Hoenes (2018); Bishop *et al.* (2010); Monteith *et al.* (2014); Taylor (1996)
fawnsurv	Fawn survival rate (F and PR; other seasons)	0.44; 0.61	Forrester and Wittmer (2013)
starv	Fawn survival to starvation rate	Eq. 3	Potapov *et al.* (2013)
survf	Yearling and adult female deer survival rate	0.85	Forrester and Wittmer (2013)
survm	Yearling and adult male deer survival rate	0.78	Bishop *et al.* (2005); Forrester and Wittmer (2013)
oldsurv	Old deer survival rate (male; female)	Eq. 4; Eq. 5	Gross and Miller (2001)
k_{hunt}	Shape parameter of gamma function for hunting pressure (adult/old male; adult/old female; yearling male; other)	12.325; 12.327; 12.331; 0	Numerically optimized from CDFW harvest statistics
θ_{hunt}	Scale parameter of gamma function for hunting pressure (adult/old male; adult/old female; yearling male; other)	$1.6 \cdot 10^{-2}$; $1.3 \cdot 10^{-4}$; $1.6 \cdot 10^{-5}$; 0	
cwdmort	Mortality rate associated with CWD infection (F and PR; other seasons)	0.11; 0.32	Miller *et al.* (2008)
cwdsol	Probability of becoming solitary when clinical CWD starts	0.64	Mejia Salazar *et al.*, 2016)
grmixed	Mixed group size (EG; PR and R)	8 – 11; 4 - 7	Mejia Salazar *et al.* (2016)
grdoe	Doe group size (EG; F, PR and R)	4 – 6; 2 - 5	Mejia Salazar *et al.* (2016)
grbuck	Buck group size (LG; F)	3 – 6; 3 - 4	Mejia Salazar *et al.* (2016)
gryearling	Yearling group size (F)	2 - 4	Mejia Salazar *et al.* (2016)
disp	Probability for a yearling to disperse (male; female)	0.6; 0.35	Robinette (1966)
disprange	Max. number of cells a deer can move for dispersion	4	Hamlin and Mackie (1989)
migrrange	Max. number of cells a deer can move for migration	10	Mackie (1998)
speed	Displacement speed (in km/day)	16	Lendrum *et al.* (2013)

Table 4. Epidemiological parameters employed for the modelling.

Parameter	Description	Value	Source
β	Within group transmission rate	0.85	Jennelle *et al.* (2014); Potapov *et al.* (2013)
β'	Environmental transmission rate	2·10-4	Jennelle *et al.* (2014)
β_c	Probability of transmission from carcass given a contact	0.037	Miller *et al.* (2004)
λ, λ_G, λ_E, λ_C	Probability of being infected each step (total; from group; from environment; from carcass)	Eq. 9-16	Jennelle *et al.* (2009); Potapov *et al.* (2013)
δ_{ff}, δ_{fm}, δ_{mf}, δ_{mm}	Interaction rate (female-female; female-male; male-female; male-male)	0.52; 1.04; 0.52; 1.91	Mejia Salazar (2017)
φ_f, φ_m, φ_{fa}	Food consumption rate (female, male, fawn)	0.93; 0.88; 1.19	Potapov *et al.* (2013)
ρ	Probability of visiting a carcass each step	$1.6 \cdot 10^{-4}$	Numerically optimized from Jennelle *et al.* (2009)
I_{fgr}, I_{mgr}, I_{fagr}	Number of infected deer within the group (females, males, fawns)		Model output
$I_{365cell}$	Number of infected deer that have been in the grid cell in the last 365 days		Model output
N_{fgr}, N_{mgr}, N_{fagr}	Number of deer within the group (females, males, fawns)		Model output
$N_{carcass}$	Number of carcasses in the grid cell		Model output
τ	Days of carcass persistence in the environment	Eq. 6-8	Numerically optimized from Jennelle *et al.* (2009)
d_i	Number of days an infected deer *i* has spent in the grid cell		Model output
βdif	Probability of CWD diffusion to a neighboring cell	Eq. 17	Model output

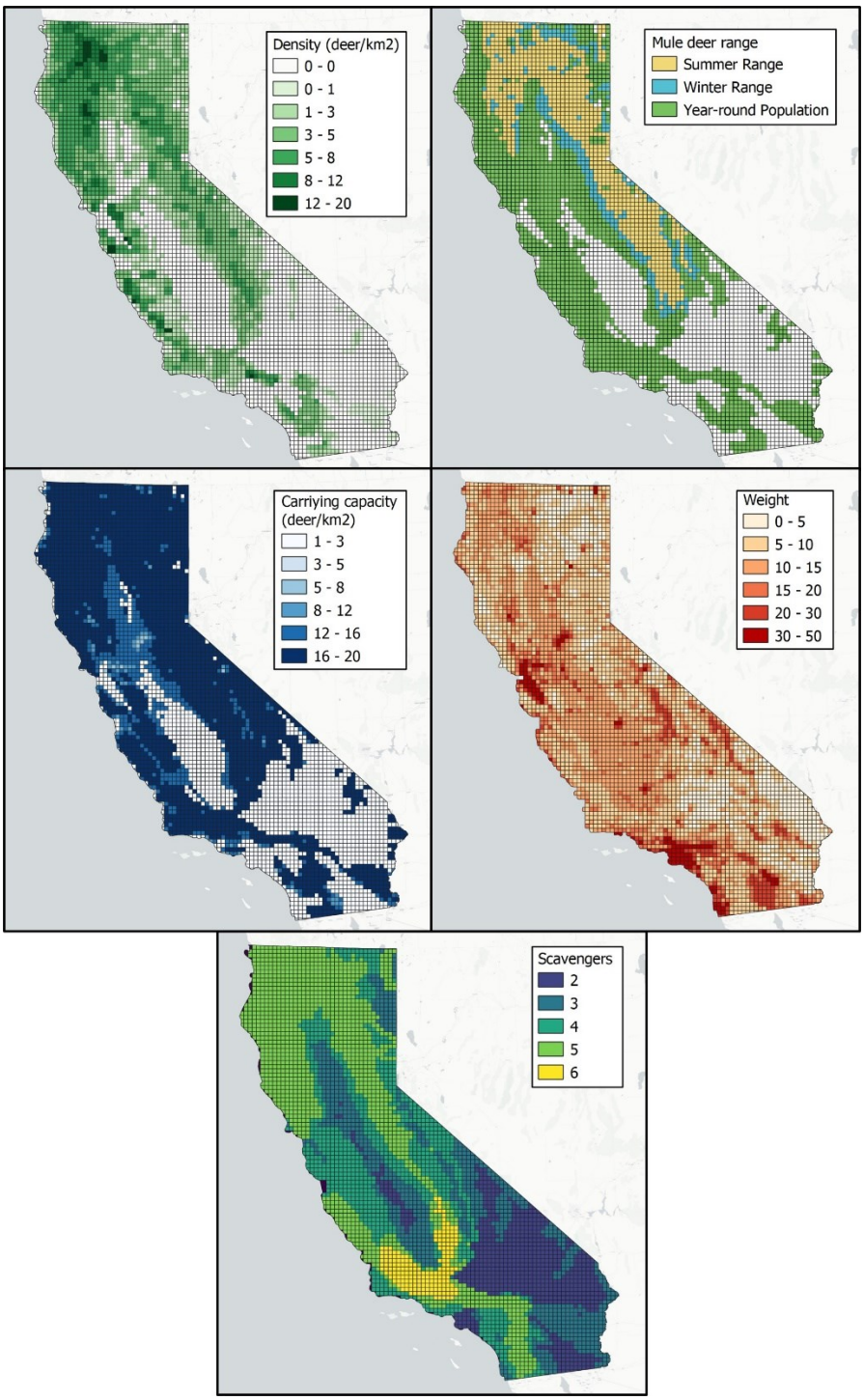

Figure 1. Initial values of the state variables of the grid cells utilized in the simulation.

The CDFW provided data on migratory corridors based on animals collared with GPS transmitters in various populations across the state. These data classified the areas used as migratory corridors by each population into three categories: standard (used by between 0 and 10% of the marked animals in that population), moderate (between 10 and 20%), and high use (more than 20%). We assigned to these areas the coefficients 1.1, 1.2 and 1.3, respectively, while the remaining portion of the State was assigned a value of 1. For each grid cell, we pondered the values by surface to obtain a parameter of use as migratory corridor (*corr*). This parameter was then combined with the *hs* parameter and the average terrain slope (*slope*) to assign a resistance value to each cell (state variable *weight*) using the following formula:

$$weight_i = (1 - hf_i) \cdot 50 + slope_i / corr_i \quad (2)$$

A *weight* value ranging from 0 to 100 is obtained for each cell. The higher the *weight*, the greater the resistance of the cell to the movement and residence of the mule deer. The objective of this approach is to encourage the majority of the deer to migrate along the same cells, thereby forming migratory corridors (Monteith *et al.* 2018), and to aggregate them in the most favorable areas during the winter months (D'Eon & Serrouya 2005).

Table 5. Drought and wildfire related parameters employed in the model.

Parameter	Description	Value	Source
droughtp	Drought probability each year	0.2	Mount, Escriva-Bou and Sencan (2021)
firep	Wildfire probability in a given cell each year	0.015	Numerically optimized from CALFIRE data
bigfirep	Probability for a wildfire of burning the neighboring cells	0.0028	Numerically optimized from CALFIRE data

2.6. Input data

The model does not use input data to represent time varying processes.

2.7. Submodels

2.7.1. Aging

Every step each deer agent increases the *age* value by 1 day. The state variable *class* changes from 1 (fawns) to 2 (yearlings) when *age* = 366 days (1 year), to 3 (adult) when *age* = 731 days (2 years), and to 4 (old) when *age* = 3286 days (9 years) for males and *age* = 4016 days (11 years) for females.

2.7.2. Natural mortality

Natural mortality occurs every step. The survival of fawns during the winter months was considered to be affected by starvation in cases where the abundance of deer is higher than the 85% of the *K* (Bergman *et al.* 2015). We employed a simple survival to starvation index (*starv*) based on Potapov *et al.* (2013):

$$starv = \min\left\{1,\quad 0.85 \cdot {K}/{N}\right\} \tag{3}$$

Consequently, the survival rate of yearlings and adults is determined by the *surv* parameter. For fawns, it results from the product of *fawnsurv* and *starv* parameters. For old deer, it is estimated as a linear decline from the *surv* value to 0 at the maximum age (Gross & Miller 2001), resulting in the following equations for males and females, respectively:

$$oldsurv_m = -0.29 \cdot {age}/{365} - 3.4 \tag{4}$$

$$oldsurv_f = -0.17 \cdot {age}/{365} - 2.72 \tag{5}$$

2.7.3. Hunting mortality

Hunting mortality occurs every step during the hunting season. The hunting pressure is calculated for each cell, age group, and sex at the beginning of

each hunting season. The probability of an individual being hunted during the season is obtained by randomly sampling from a gamma distribution Γ (k_{hunt}, θ_{hunt}). This probability is then divided over the 85 days of the hunting season to obtain the probability of being hunted at each step.

2.7.4. CWD mortality

Miller *et al.* (2008) observed that deer infected with CWD were more susceptible to death from causes not directly related to the disease, such as hypothermia or predation. In their study, the diagnosis of CWD was performed using immunohistochemical staining, which allows for the preclinical detection of CWD in mule deer between 6 and 12 months after infection (Haley *et al.* 2012). Given that prion shedding commences 6-9 post-infection (Plummer *et al.* 2017; Tamguney *et al.* 2009), we considered an increase of *cwdmort* in mortality for infectious deer. All infected deer die 504 to 610 days after infection (Johnson *et al.* 2011; Williams 2005).

2.7.5. Carcass removal

When a deer infected with CWD dies, its carcass remains infectious in the environment until it decomposes or is consumed as carrion (Miller *et al.* 2004). Jennelle *et al.* (2009) assessed the persistence of deer carcasses in the environment concluding that season and scavenging pressure are the primary determinants. We used the data collected in their research to estimate de carcass survival (τ) for the four scheduled seasons considering the number of main scavenger species present (*scvg*;):

$$\tau_{PR\ and\ R} = 33.78^{-0.27 \cdot scvg} \quad (6)$$

$$\tau_{EG} = 63.24^{-0.06 \cdot scvg} \quad (7)$$

$$\tau_{LG\ and\ F} = 71.21^{-0.24 \cdot scvg} \quad (8)$$

Black bear (*Ursus americanus*), mountain lion (*Puma concolor*), coyote (*Canis latrans*), California condor (*Gymnogyps californianus*), turkey vulture (*Cathartes aura*), and the feral pig (*Sus scrofa*) were considered as potential scavengers of mule deer carcasses (Allen *et al.* 2015; 2021; Bauer *et al.* 2005; Jennelle *et al.* 2009). The information about the presence of these species was provided by the CDFW.

2.7.6. Fawning

During EG season, each female deer older than 548 days (1.5 years) has *preg* probability of fawning. In case of fawning, it has *twinp* probability of giving birth to twins. Sex ratio at birth is determined by the *fawnsex* parameter.

2.7.7. Group dynamics

During PR and R periods, females without fawns are in groups of size *grdoe,* and males are in mixed groups of size *grmixed* with females and fawns. At the beginning of EG, small doe groups and mixed groups join to form larger groups of sizes *grdoe* and *grmixed,* respectively. In LG period, adult and old males leave the mixed groups to form male groups of size *grbuck*. During F season, pregnant females separate and give birth, forming groups with their fawns. Yearlings separate and form their own groups of size *gryearling*. When the yearly cycle comes to an end and the PR period begins again, male and yearling groups join females with fawns forming mixed groups of size *grmixed,* and females without fawns remain in groups of size *grdoe.*

2.7.8. Dispersal

When the time comes for dispersal, each yearling deer has *disp* probability for dispersion. If $N \geq 0.7 \cdot K$ in the grid cell where the deer is located, the probability of dispersal is 1. When a deer disperses, it moves to the nearest grid

cell in which $N \leq 0.7 \cdot K$ in a *disprange* range of cells around its starting grid cell. Cells outside the summer or year-round range are discarded. If there are no cells in *disprange* that meet the aforementioned conditions, the deer will move to the cell with the least *weight* in *disprange*. Movements were assumed to follow the principle of least effort (Zipf 1949), which means that displacements occur through the cells with a lower *weight* value. The speed of movement is determined by the *speed* parameter.

2.7.9. Migration

As the fall migration period begins, all migratory deer move from their cells in the summer range to a randomly selected cell in the winter range that meets $N \leq 0.8 \cdot K$ within a *migrrange* range of cells around its starting grid cell. Therefore, they do not necessarily migrate to the same area every year (van de Kerk *et al.* 2021). Migrations occur in groups (Shellard & Mayor 2020), with all deer belonging to the same group migrating to the same cell. If there are no cells in a *migrrange* distance that meet this condition, the deer will move to the cell with the least *weight* in the winter range in a the *migrrange* range of cells. In spring migration, all migratory deer moves from its cell in the winter range to the cell where it was located before fall migration. Displacements occur through the cells with the lower *weight* values at a speed determined by the *speed* parameter.

2.7.10. Carrying capacity dispersal

The model assumes that when $N > 0.9 \cdot K$ in a cell, a dispersal process begins as a result of intraspecific competition for available resources (Valente *et al.* 2020). In a cell where this condition is met, the probability of a deer leaving the cell at each step (P_k) is determined as follows:

$$P_k = {0.1 \cdot (N - 0.9 \cdot K)}/{0.9 \cdot K} \quad (9)$$

This process causes the population to fluctuate slightly around the K of the cell. When a deer leaves the cell, it moves to the nearest grid cell where $N \leq 0.7 \cdot K$ in a *disprange* range of cells around its starting grid cell. The target cell must belong to the same seasonal range as the starting cell (summer or winter) or be a year-round range cell. If there are no cells in *disprange* that meet these conditions, it moves to the cell with the least *weight* in *disprange*. The deer move through the cells with the lower *weight* value at a speed determined by the *speed* parameter.

2.7.11. CWD Force of infection

CWD transmission may be frequency-dependent (FD) density-dependent (DD), or a combination of both (Grear *et al.* 2010; Jennelle *et al.* 2014; Storm *et al.* 2013; Winter & Escobar 2020). FD within-group transmission is considered to be the main mechanism of CWD transmission (Potapov *et al.* 2013; 2016; Storm *et al.* 2013). However, intergroup environmental transmission, which is a DD mechanism, has been shown to play a role in the disease dynamics, especially after a long period of time when the disease becomes endemic (Almberg *et al.* 2011; Miller, Hobbs & Tavener 2006). Therefore, we considered both within-group transmission and environmental transmission between groups, excluding FD transmission between groups since direct contacts between groups are rare and the likelihood of infection from a single contact is low (Belsare & Stewart 2020; Habib *et al.* 2011; Kjaer 2010). We also considered the possibility of transmission from an infectious carcass (Miller *et al.* 2004). Thus, the probability of becoming infected at each step for a given individual is determined by the probability of becoming infected by another individual of the same group (λ_G), the probability of becoming infected by the environment (λ_E), and the probability of becoming infected by an infectious carcass (λ_C).

2.7.11.1. Transmission rates (β and β′)

Actual values of transmission rates for mule deer in California are not available, although estimates have been made for other populations and species have been carried out (Almberg *et al.* 2011; Jennelle *et al.* 2014; Miller, Hobbs & Tavener 2006; Potapov *et al.* 2016; Wasserberg *et al.* 2009). CWD prevalence rates in males can be up to twice as high as in females, and lower in yearlings (Edmunds *et al.* 2016; Heisey *et al.* 2010b; Osnas *et al.* 2009), leading Jennelle *et al.* (2014) to suggest a different transmission rate for males and females as the most plausible option in their study of white-tailed deer (*Odocoileus virginianus*). However, higher prevalence in males and adults is likely associated with consumption and interaction behavior (Potapov *et al.* 2013), which may vary between species. Consequently, we decided to use sex-independent transmission rates of $\beta = 0.85$ infections·year^{-1} (Jennelle *et al.* 2014; Potapov *et al.* 2016) for within-group transmission and $\beta' = 2 \cdot 10^{-4}$ infections·year^{-1}·individual^{-1} (Jennelle *et al.* 2014) for environmental transmission, and combine them with parameters related to food consumption and interaction rates.

2.7.11.2. Probability of group infection (λ_G)

For the within-group transmission, we included a parameter related to interaction rates (δ), with higher values assigned to males than to females and fawns (Mejia Salazar 2017). The probability of an individual being infected by a group member each time step for females (*f*), males (*m*) and fawns (*fa*) is calculated as follows:

$$\lambda_{Gf} = \beta/_{365} \cdot \delta_{mf} \cdot \frac{I_{mgr}}{N_{mgr}} + \beta/_{365} \cdot \delta_{ff} \cdot \frac{I_{fgr} + I_{fagr}}{N_{fgr} + N_{fagr}} \quad (10)$$

$$\lambda_{Gm} = \beta/_{365} \cdot \delta_{mm} \cdot \frac{I_{mgr}}{N_{mgr}} + \beta/_{365} \cdot \delta_{fm} \cdot \frac{I_{fgr} + I_{fagr}}{N_{fgr} + N_{fagr}} \quad (11)$$

$$\lambda_{Gfa} = {}^{\beta}/_{365} \cdot \delta_{mf} \cdot \frac{I_{mgr}}{N_{mgr}} + {}^{\beta}/_{365} \cdot \delta_{ff} \cdot \frac{I_{fgr} + I_{fagr}}{N_{fgr} + N_{fagr}} \quad (12)$$

2.7.11.3. Probability of environmental infection (λ_E)

Although CWD prion can be found in the soil and plants for a long time after excretion (Mathiason *et al.* 2009; Miller *et al.* 2004; Plummer *et al.* 2018), Miller *et al.* (2004) reported a rapid rate of removal of the amount of prions from the environment. Potapov *et al.* (2013) evaluated the impact of infected deer in the past, concluding that the effect is weak and justifying the assumption of one year of pathogen survival in the environment. Consequently, we calculated the probability of infection from an environmental source of prions for a given deer at each step considering the sum of days that every excreting deer spent in the grid cell during the previous 365 days. A food parameter related to food consumption (φ) was also included:

$$\lambda_{Gf} = {}^{\beta'}/_{365} \cdot \varphi_f \cdot \sum_{i=1}^{I_{365cell}} d_i \quad (13)$$

$$\lambda_{Gm} = {}^{\beta'}/_{365} \cdot \varphi_f \cdot \sum_{i=1}^{I_{365cell}} d_i \quad (14)$$

$$\lambda_{Gfa} = {}^{\beta'}/_{365} \cdot \varphi_{fa} \cdot \sum_{i=1}^{I_{gridcell-365\ days}} d_i \quad (15)$$

2.7.11.4. Probability of carcass infection (λ_C)

The transmission from infectious deer carcasses to healthy deer has already been proven (Miller *et al.* 2004). Furthermore, the nutrient supply from the carcass to the soil leads to an increase in vegetation, entailing attraction effect for ungulates (Towne 2000; Walker *et al.* 2020). However, transmission from

carcasses is usually overlooked in CWD epidemiological studies. We used the data collected by Jennelle *et al.* (2009) to estimate the probability of a given deer in a cell visiting a carcass at each step (ρ), which was then combined with the probability of infection through contact with a carcass (β_C) estimated by Miller *et al.* (2004). Consequently, the probability of infection by a carcass present in the grid cell at each step can be estimated. When combined with the number of carcasses present in the grid cell ($N_{carcass}$), this leads to the probability of infection from carcasses at each step.

$$\lambda_C = \beta_C \cdot \rho \cdot N_{carcass} \quad (16)$$

2.7.12. CWD Diffusion

The discretization of space into a grid signifies that the only way an individual in a cell other than the outbreak cell can become infected is through the arrival of an infected individual, either by dispersal or migration. Since individuals at the edge of a cell could come into contact and form groups with individuals from neighboring cells, thereby spreading the pathogen, a diffusion model is also added to the simulation. The spread rate is typically between 5 and 10 km per year from a focus of all infected individuals (Garlick *et al.* 2014; Xu, Merrill & Lewis 2022). In our grid, this would imply that from a cell where all individuals are infected, all 8 neighboring cells would also be infected within a year. The lower the prevalence, the lower the probability of neighboring cells becoming infected. For the diffusion model, we assume that the relationship between prevalence and the probability of diffusion is linear. Xu, Merrill and Lewis (2022) observed a correlation between the density of deer groups and the speed of spread, since a higher number of groups increases the likelihood of contact between them. Based on their calculations, we assumed that there is a linear relationship between the speed of expansion and the density of deer groups present, from 1.5 km/year (which would take approximately 5 years to spread to neighboring cells) for 1 group per 100 km², to 7.5 km/year (which would take approximately 1 year) for

100 groups per 100 km². Consequently, for each infected cell *i* (i.e., with at least one infected individual) with *Ngr* deer groups inside, the probability (*βdif*) of an individual in a neighboring cell *z* becoming infected at each step is calculated as follows:

$$\beta dif_z = prevalence_i \cdot (0.2 + 0.008 \cdot Ngr_i)/365 \quad (17)$$

2.7.13. Droughts

Every year there is a probability *droughtp* that an interannual drought will begin, lasting between 365 and 1460 days (1 to 4 years; Miller *et al.* 2022). The drought covers the entire State of California resulting in an increase in mortality rates by 15% (Jackson *et al.* 2021; Schuyler, Dugger & Jackson 2018) and in the probability of wildfires by 40% (Littell *et al.* 2016; Madadgar *et al.* 2020). Furthermore, a 25% reduction in *K* is also considered.

2.7.14. Wildfires

Each cell has a probability *firep* of undergoing a wildfire during the summer. Similarly, each wildfire has a probability *bigfirep* of spreading the wildfire to the neighboring cells. When a cell burns out, it is assumed that the environmental prion load is removed by high temperatures (Lee 2023), signifying that $\sum_{i=1}^{I_{365cell}} d_i = 0$ (see Equations 13-15).

Furthermore, an effect on *K* of the cell is considered (Bristow *et al.* 2020; Sparks *et al.* 2018). This effect is observed to decrease to a minimum during the first year after the fire (5%), increase over the second year due to the growth of low vegetation (190%), and stabilize from the third and fourth years (90%) before returning to its original value from the fifth year after the wildfire. The substantial reduction in *K* due to a fire initiates a dispersion process (see Equation 9), in which a large difference between *N* and *K* would result in the vast majority of deer in the cell fleeing ahead in a very short time (van Mantgem, Keeley & Witter 2015).

3. Model evaluation

The ecological module of the model was evaluated through long-term population trends. In California, mule deer populations have been slightly declining for several decades (Loft & Bleich 2014; Webb 2013). To ensure that this pattern was reflected in the model, 20 iterations were conducted over a simulation of 50 years (18,250 steps) with a population of 10,000 deer in an area of 41,000 km^2 covering all mule deer ranges (summer, winter and year-round). These simulations were performed without initiating CWD outbreaks, in order to assess the population dynamics in the absence of the pathogen. The simulations showed a slight decline in the mule deer population over a 50-year period, with an average abundance of 8,370 individuals across the 20 iterations (ranging from 6,326 to 11,166) at the end of the simulation (see Figure 2). This outcome aligns with the observed population pattern of mule deer in California over the past few decades (Loft & Bleich 2014; Webb 2013).

The epidemiological module is more challenging to evaluate due to the lack of empirical data on the prevalence and distribution of the disease in California. Observed patterns in CWD dynamics indicate a higher prevalence in bucks (adult and old males) than in does (adult and old females) and yearlings (Edmunds *et al.* 2016; Grear *et al.* 2006; Miller & Conner 2005; Osnas *et al.* 2009) and a spread velocity between 3.7 and 11 km/year (Garlick *et al.* 2014; Xu, Merrill & Lewis 2022). Consequently, the model's results were evaluated through these patterns. To this end, 5 iterations of simulations lasting 7 years and 9 months (2,828 steps) were conducted, with a population of 625,000 mule deer in the entire state of California based on the best available data (CDFW 2024a), resulting in 46,160 deer in the area of 41,000 km^2 considered for the simulation. The outbreaks were initiated on May 1st, as this is the month when the first cases have been detected (Munk & Benedet 2024). This is 9 months after the start of the simulation on August 1st, signifying 7 years of pathogen spread simulation. The outbreaks were initiated in a non-migratory population to avoid the potential impact of

migratory movements on the spatial dynamics of the pathogen, since such movements could influence the spread rate or prevalence rates.

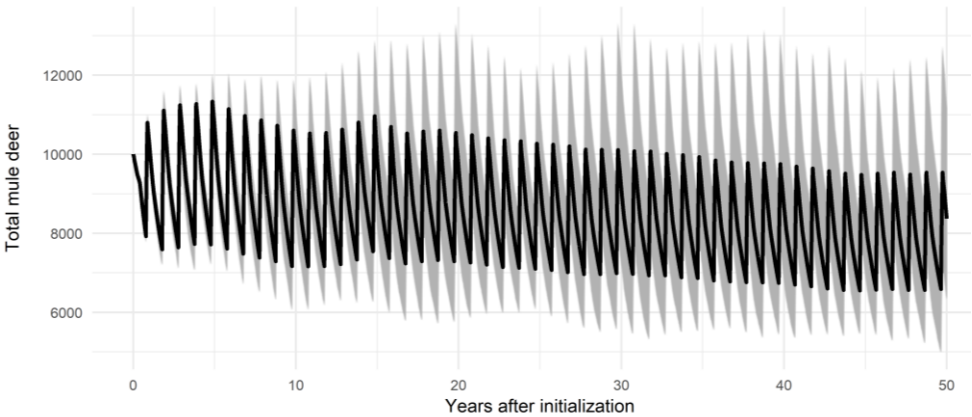

Figure 2. Evolution of the total number of mule deer over a 50-year simulation. The initial population was 10,000 deer in an area of 41,000 km². The black line represents the average value across 20 iterations, while the gray shading represents the maximum and minimum values.

As a result, CWD exhibited an average spread of 50 km across the 10 iterations (ranging from 48 to 53 km) over the 7 years, resulting in an average spread rate of 7.1 km/year (ranging from 6.9 to 7.6 km/year). This value is consistent with the expected rates observed in previous studies (3.7 to 11 km/year in Garlick *et al.* 2014; 7.3 km/year in Xu, Merrill & Lewis 2022). The prevalence of CWD was found to be higher in bucks than in does and yearlings in all iterations, with a the exception of one iteration where the prevalence in does was slightly higher (4.81% compared to 4.48%, see Table 6), as expected by previously reported values (Edmunds *et al.* 2016; Grear *et al.* 2006; Miller & Conner 2005). The prevalence of CWD in fawns was indeed higher than expected based on previously reported values (Heisey *et al.* 2010b; Osnas *et al.* 2009). However, the few data regarding prevalence rates in fawns pertain to populations of a different species (white-tailed deer) in areas where CWD is endemic, and the disease dynamics may differ.

Iteration	Accumulated exposed mule deer	Prevalence rates (whole simulation area)			
		Bucks	Does	Yearlings	Fawns
1	2,884	4.48 %	4.81 %	3.78 %	4.78 %
2	2,890	8.71 %	8.52 %	7.87 %	9.76 %
3	2,143	7.88 %	6.29 %	5.71 %	7.23 %
4	2,171	3.54 %	3.20 %	2.77 %	3.91 %
5	2,289	5.75 %	4.99 %	4.62 %	5.98 %

Table 6. Accumulated exposed mule deer and CWD prevalences by sex and age class over 7 years of pathogen presence in an initial population of 46,160 mule deer in an area of 41,000 km², with the outbreak initiating in a non-migratory population. The values at the end of the simulation are shown for the 5 iterations.

Therefore, the demographic patterns of mule deer populations and the epidemiological patterns of CWD are shown to be within the expected range based on previous observational studies. Thus, the model's parameterization is shown to be reliable, lending credibility to the potential emergence of spatiotemporal patterns derived from the model.

Supporting Information

Introduction

Some of the parameters included in the modeling were estimated based on information derived from previous scientific research and reports published by the California Department of Fish and Wildlife (CDFW) and the California Department of Forestry and Fire Protection (CALFIRE). This document provides an account of the processes employed to obtain these parameters.

1. Hunting pressure (k_{hunt}, ϑ_{hunt})

Hunting pressure was estimated based on mule deer population estimates and hunting statistics reports from CDFW. These reports are publicly available online at https://wildlife.ca.gov/Conservation/Mammals/Deer/Population and https://wildlife.ca.gov/Hunting/Deer respectively. In order to ascertain the distribution of hunting pressure by age and sex classes, the percentage of hunted mule deer corresponding to male yearlings, adult/old females (does), and adult/old males (bucks) was calculated based on the data included in the hunting statistics reports which included the information categorized by sex and age class, spanning from 2013 to 2017 (see Table S1).

Year	Yearling males	Does	Total	% Yearling males	% Does	% Males
2013	22	324	14,703	0.1	2.2	97.6
2014	14	282	14,199	0.1	2.0	97.9
2015	18	334	19,639	0.1	1.7	98.2
2016	22	442	27,608	0.1	1.6	98.3
2017	29	394	21,749	0.1	1.8	98.1
			Average	0.1	1.9	98.0

Table S1. Hunting statistics for the entire state of California by sex and age class between the years 2013 and 2017.

Table S2. Hunting statistics for each mule deer game management area in California.

Hunting Zone	Abundance proportion	Deer abundance	Buck abundance	Doe abundance	Male yearling abundance	Mean hunted deer (2013 – 2017)	Hunting pressure bucks	Hunting pressure Does	Hunting pressure male yearlings
A	0.2441	305,115	33,563	91,535	33,563	7,923	0.2313560	0.0016447	0.0002361
B1	0.0776	97,056	10,676	29,117	10,676	2,731	0.2507064	0.0017822	0.0002558
B2	0.0617	77,144	8,486	23,143	8,486	2,435	0.2812340	0.0019992	0.0002870
B3	0.0148	18,550	2,041	5,565	2,041	537	0.2580933	0.0018347	0.0002634
B4	0.0102	12,726	1,400	3,818	1,400	353	0.2468463	0.0017548	0.0002519
B5	0.0203	25,433	2,798	7,630	2,798	707	0.2477257	0.0017610	0.0002528
B6	0.0266	33,211	3,653	9,963	3,653	1,003	0.2690059	0.0019123	0.0002745
C1	0.0170	21,256	2,338	6,377	2,338	412	0.1726837	0.0012276	0.0001762
C2	0.0100	12,553	1,381	3,766	1,381	351	0.2493943	0.0017729	0.0002545
C3	0.0127	15,830	1,741	4,749	1,741	445	0.2503392	0.0017796	0.0002554
C4	0.0498	62,273	6,850	18,682	6,850	834	0.1193453	0.0008484	0.0001218
D3	0.0707	88,419	9,726	26,526	9,726	2,132	0.2148399	0.0015273	0.0002192
D4	0.0223	27,934	3,073	8,380	3,073	632	0.2015636	0.0014329	0.0002057
D5	0.0698	87,265	9,599	26,180	9,599	2,071	0.2114740	0.0015033	0.0002158
D6	0.0352	44,035	4,844	13,211	4,844	907	0.1835822	0.0013051	0.0001873
D7	0.0260	32,451	3,570	9,735	3,570	710	0.1950312	0.0013864	0.0001990
D8	0.0162	20,229	2,225	6,069	2,225	518	0.2280419	0.0016211	0.0002327

Table S2 cont.

Hunting Zone	Abundance proportion	Deer abundance	Buck abundance	Doe abundance	Male yearling abundance	Mean hunted deer (2013 – 2017)	Hunting pressure bucks	Hunting pressure Does	Hunting pressure male yearlings
D9	0.0113	14,085	1,549	4,225	1,549	232	0.1464952	0.0010414	0.0001495
D10	0.0047	5,872	646	1,762	646	140	0.2130056	0.0015142	0.0002174
D11	0.0133	16,638	1,830	4,991	1,830	487	0.2608757	0.0018545	0.0002662
D12	0.0074	9,226	1,015	2,768	1,015	157	0.1518071	0.0010792	0.0001549
D13	0.0097	12,073	1,328	3,622	1,328	356	0.2628537	0.0018686	0.0002682
D14	0.0111	13,902	1,529	4,171	1,529	402	0.2577548	0.0018323	0.0002630
D15	0.0064	7,983	878	2,395	878	82	0.0912905	0.0006490	0.0000932
D16	0.0160	19,978	2,198	5,993	2,198	459	0.2046046	0.0014545	0.0002088
D17	0.0084	10,470	1,152	3,141	1,152	133	0.1128264	0.0008021	0.0001151
D19	0.0054	6,712	738	2,014	738	161	0.2131657	0.0015154	0.0002175
X1	0.0121	15,174	1,669	4,552	1,669	371	0.2180585	0.0015501	0.0002225
X2	0.0040	4,980	548	1,494	548	115	0.2064371	0.0014675	0.0002107
X3a	0.0066	8,254	908	2,476	908	174	0.1882369	0.0013381	0.0001921
X3b	0.0129	16,080	1,769	4,824	1,769	363	0.2011210	0.0014297	0.0002052
X4	0.0076	9,475	1,042	2,843	1,042	215	0.2025321	0.0014398	0.0002067
X5a	0.0015	1,882	207	565	207	40	0.1912099	0.0013593	0.0001951
X5b	0.0017	2,152	237	645	237	39	0.1631488	0.0011598	0.0001665
X6a	0.0069	8,639	950	2,592	950	211	0.2171950	0.0015440	0.0002216

Table S2 cont.

Hunting Zone	Abundance proportion	Deer abundance	Buck abundance	Doe abundance	Male yearling abundance	Mean hunted deer (2013 – 2017)	Hunting pressure bucks	Hunting pressure Does	Hunting pressure male yearlings
X6b	0.0067	8,423	926	2,527	926	155	0.1639525	0.0011655	0.0001673
X7a	0.0048	6,029	663	1,809	663	113	0.1669881	0.0011871	0.0001704
X7b	0.0028	3,470	382	1,041	382	65	0.1679218	0.0011937	0.0001713
X8	0.0019	2,404	264	721	264	56	0.2067651	0.0014699	0.0002110
X9a	0.0175	21,881	2,407	6,564	2,407	304	0.1238557	0.0008805	0.0001264
X9b	0.0101	12,566	1,382	3,770	1,382	125	0.0887682	0.0006310	0.0000906
X9c	0.0057	7,148	786	2,144	786	113	0.1405992	0.0009995	0.0001435
X10	0.0045	5,639	620	1,692	620	55	0.0872043	0.0006199	0.0000890
X12	0.0139	17,384	1,912	5,215	1,912	270	0.1385755	0.0009851	0.0001414

The proportion of the population in each hunting area was calculated using population estimates, with a total population value of 1,250,000 deer throughout the state (B. Munk & A. Hereen, unpublished data). The number of male yearlings, does, and bucks was estimated based on the proportions shown in Table 2 of the main text. The number of hunted individuals in each hunting area was calculated by multiplying the number of individuals hunted over the period by the proportions shown in Table S2, and then divided by the abundance of their sex and age class to obtain the hunting pressure on each age and sex class for each game management area (see Table S2). A Gamma distribution Γ (k, θ) was employed to fit the hunting pressure for each sex and age class (see Figure S1). The hunting pressure in each cell is calculated annually by sampling from each of these Gamma distributions, thereby introducing spatial and temporal stochasticity to the hunting pressure. The increases in mortality of old and adult male deer resulting from the calculated hunting pressure are consistent with data derived from studies conducted in other areas (Bishop *et al.* 2005; Forrester & Wittmer 2013).

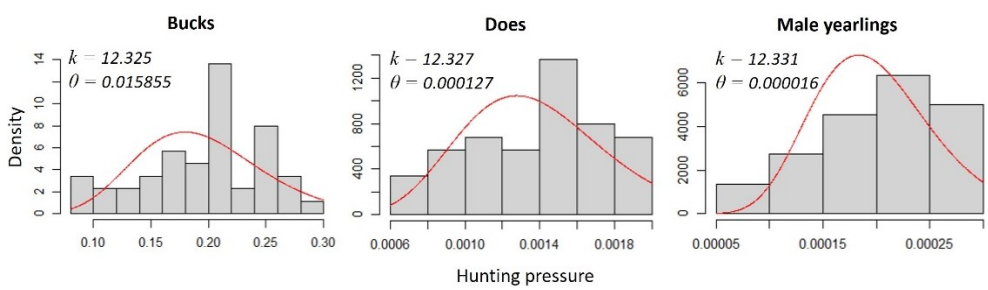

Figure S1. Gamma fitting to the mule deer hunting pressure values from the different game management areas of California.

2. Probability of visiting a carcass (ρ)

Jennelle *et al.* (2009) observed an average of 0.24 visits per day by white-tailed deer (*Odocoileus virginianus*) to carcasses of the same species. The study

was conducted in an area of 544 km², with a mean deer density of 14.5 individuals per km². This would signify an approximate abundance of 7,888 deer throughout their study area. Given the aforementioned visit frequency, the probability of each deer visiting a single carcass in 544 km2 would be 0.24/7888 = 3.10-5. If the carcass were located in the more restricted space of 100 km^2 by a cell of the grid utilized in the model, the probability would be $\rho = 3 \cdot 10^{-5} \cdot 544/100 = 1.6 \cdot 10^{-4}$.

3. Carcass duration in the environment (τ)

In the same study, Jennelle *et al.* (2009) evaluated the persistence of deer carcasses in the environment, concluding that season and scavenging pressure are the primary determinants. To estimate the persistence of carcasses (τ) for the four scheduled seasons, we fitted an exponential regression to the data collected in their research in each season (see Figure S2):

$$\tau_{PR\ and\ R} = 33.78^{-0.27 \cdot scvg}$$

$$\tau_{EG} = 63.24^{-0.06 \cdot scvg}$$

$$\tau_{LG\ and\ F} = 71.21^{-0.24 \cdot scvg}$$

Where *PR* is the pre-rut period, *R* is the rut period, *EG* is the early gestation period, *LG* is the late gestation period, *F* is the fawning period, and *scvg* is the number of scavenging species present.

The resulting persistence of a carcass in the environment for each season of the year and number of scavenging species included in the model is shown in Table S3.

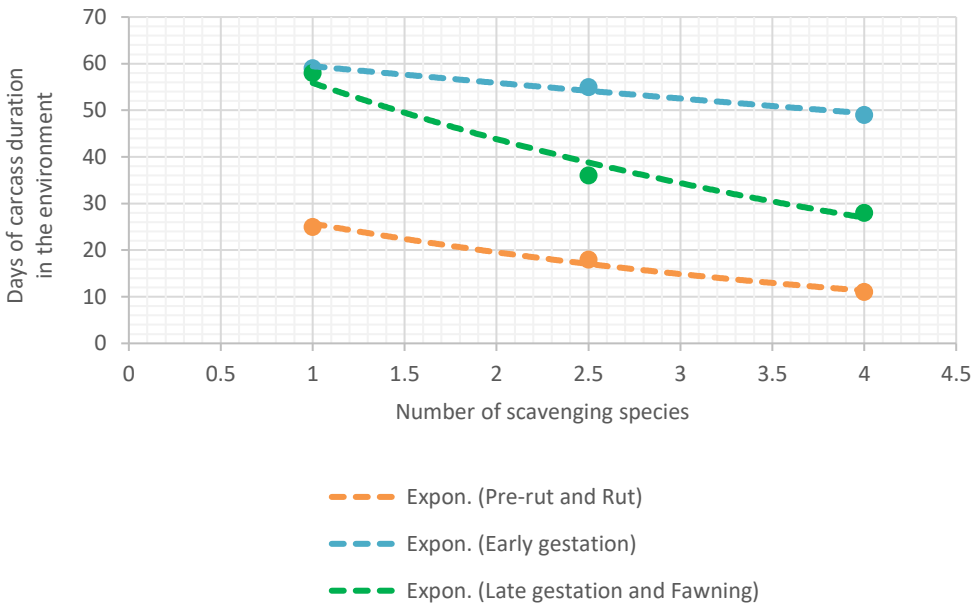

Figure S2. Exponential fitting to the data on carcass persistence in the environment collected by Jennelle *et al.* (2009).

Table S3. Duration of a deer carcass in the environment for each season and each number of scavenging species included in the model.

Number of scavenging species	Pre-rut and Rut	Early gestation	Late gestation and fawning
2	20	56	44
3	15	53	34
4	11	49	27
5	9	46	21
6	7	44	17

4. Wildfire and big fire probability (*firep* and *bigfirep*)

To estimate the probability of a cell burning each year (*firep*) and the probability that, given a fire, it becomes a large-scale fire (*bigfirep*), we utilized the CALFIRE incident database, which provides accurate information on fires that

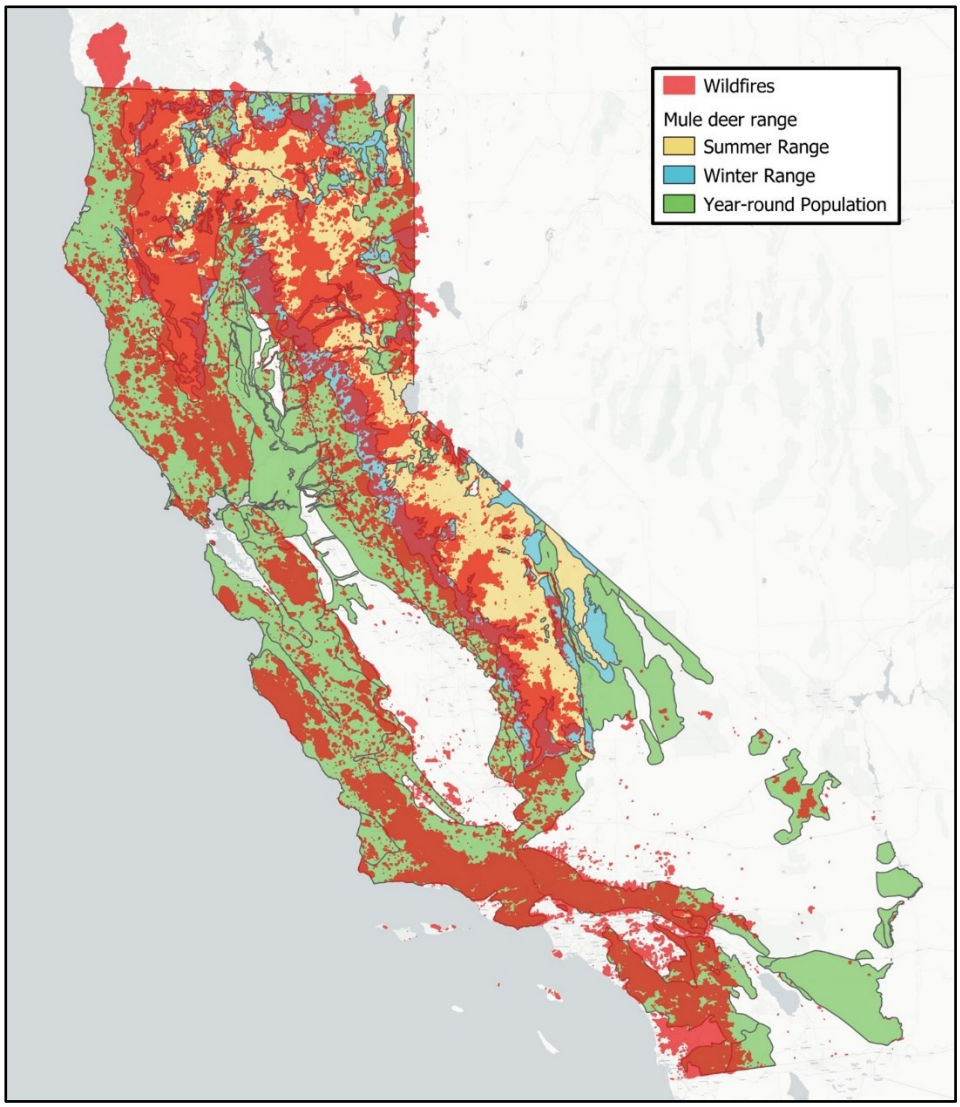

Figure S3. Area burned by historic wildfires in California, along with the distribution of mule deer. Compiled from data provided by CALFIRE and CDFW.

have occurred since 2013 to the present (available online at https://www.fire.ca.gov/incidents). We excluded fires that burned an area smaller than 1 km² as they are not expected to have a significant effect on mule deer due to their mobility and home range (van Mantgem, Keeley & Witter 2015). The remaining fires with complete year information (from 2013 to 2023) were

considered. The resulting total burned area was 43,215.5 km² over 11 years, signifying an average of 3,928.7 km² burned each year. Given that each grid cell has an area of 100 km², this would result in 3,928.7/100 = 393 cells burned each year. The majority of these fires occur within the mule deer distribution area in California (see Figure S3), which represents 25,580 cells in the grid used in the model. Consequently, if the number of cells expected to burn each year is divided by the total number of cells that can burn, a yearly fire probability in each cell is obtained, which is *firep* = 393/25,580 = 0.015.

To calculate the probability of a fire becoming a large fire that burns the 8 neighboring cells (*bigfirep*), the number of fires larger than 800 km^2 (8 cells) was counted for the period from 2013 to 2023. A total of 12 fires were counted over 11 years, averaging 1.1 large fires per year. Given that 393 fires were calculated in cells each year, the probability of each of them becoming a large fire and burning the 8 neighboring cells would be *bigfirep* = 1.1/393 = 0.0028.

Chapter 4.2: What's next? Simulating chronic wasting disease spread in California after the outbreak

Herraiz, C., González-Crespo, C., Munk, B., Heeren, A., Acevedo, P., & Martínez-López, B. What's next? Simulating chronic wasting disease spread in California after the outbreak (*in prep*.).

Abstract

Chronic Wasting Disease (CWD) is a prion-induced transmissible spongiform encephalopathy affecting cervids, leading to neurological deterioration and death. First identified in Colorado in the 1960s, CWD has since spread across North America and beyond, causing significant ecological and socio-economic impacts. The recent detection of CWD in California, previously considered CWD-free, has heightened the need for effective monitoring and control strategies. This study implements the CalCWD model, an agent-based model developed to simulate the spatiotemporal dynamics of CWD in California's mule deer populations. The model incorporates ecological and epidemiological processes to provide spatially explicit simulations of CWD spread. Ecological processes are related to demography, social structure, behavior and environment. Epidemiological processes model pathogen transmission through within-group contact, environmental prion load, and contact with infectious carcasses. Simulations were conducted to assess the risk of CWD spread from the two detected case locations in Inyo and Madera counties for a period of three years. The simulations revealed that the Inyo County outbreak, affecting a migratory deer population, poses a higher risk of pathogen spread, potentially reaching the Nevada state border within 2.25 years. The Madera County outbreak, affecting a non-migratory population, exhibited slower spread, with a mean velocity of 6.7 km per year. The results suggest that disease monitoring and control measures should be focused on Inyo County, and that surveillance at Benton and Mono valleys should be conducted to detect the potential spread into the CWD-free state of Nevada. Additionally, the model revealed that transmission through infectious carcasses is a negligible route of transmission, highlighting that control measures should focus on the hosts. The CalCWD model offers valuable insights into the potential spread of CWD in California, highlighting high-risk areas and guiding wildlife management in implementing effective monitoring and control measures.

Keywords: Agent-based model, California, chronic wasting disease, disease spread, ecological modeling, epidemiological modeling, mule deer, simulation, wildlife epidemiology

1. Introduction

Chronic Wasting Disease (CWD) is a Transmissible Spongiform Encephalopathy (TSE) caused by the PrP^{CWD} prion, which affects various species of the deer family, causing them neurological symptoms and ultimately death (Haley & Hoover 2015; Otero *et al.* 2021). Since its detection in the 1960s in Colorado (Williams & Young 1980), it has spread both across North America and to other continents (Escobar *et al.* 2020). CWD brings socio-economic problems derived from its devastating effects on captive deer and can even lead to the decline of natural populations (DeVivo *et al.* 2017; Edmunds *et al.* 2016). This has led to the monitoring and control of CWD becoming a priority for wildlife management authorities in areas where it is present (Thompson *et al.* 2023).

California was considered CWD-free. Recently, two cases were detected in two different areas of California in May 2024 (NWHC 2024). The route of entry into the state is currently unknown. However, given that the neighboring states of Oregon and Nevada are CWD-free (NWHC 2024), the most probable route is through hunters from California who hunt in states where the disease is prevalent and bring carcasses for meat processing and/or taxidermy (Ableman *et al.* 2019; Feltman *et al.* 2023). The existence of mule deer migratory corridors between California and the aforementioned neighboring states renders the state of California a potential focal point for the expansion of CWD in the western United States (Ahlborn & White 2006; Farnsworth *et al.* 2006; Monteith *et al.* 2011). The California Department of Fish and Wildlife (CDFW) has called for collaboration with hunters, taxidermists and meat processing centers to obtain samples in these areas (Munk & Benedet 2024). However, the uneven distribution in age and sex classes of both the disease and the samples obtained from hunting makes it difficult to obtain representative samples of the population's health status. Furthermore, the long incubation periods of the pathogen, ranging from several months to even years (Johnson *et al.* 2011; Williams 2005), the survival of the pathogen in infectious form in the environment and in the carcasses of infected

individuals (Jennelle *et al.* 2009; Miller *et al.* 2004), and the low prevalences during the early years after the emergence of the disease (Mysterud & Edmunds 2019) make both early detection and spread monitoring after the outbreak challenging (Evans, Schuler & Walter 2014; Thompson *et al.* 2023).

Agent-based models (ABMs) employ a bottom-up approach, whereby processes occurring at the individual, group, or local scale are parameterized and then scaled up to broader patterns and dynamics (Grimm *et al.* 2005; Macy & Willer 2002). This enables the simulation of the spread of a pathogen in a location where it has just emerged, based on the host's demographic parameters and epidemiological dynamics observed in the disease in other areas (Lane-deGraaf *et al.* 2013; Marion *et al.* 2008). Consequently, it is possible to predict the locations where the pathogen is most likely to spread, thereby assisting managers in directing sampling efforts and control measures (Belsare *et al.* 2020b; Dion, VanSchalkwyk & Lambin 2011; Potapov *et al.* 2016).

The CalCWD is an agent-based model developed on the GAMA platform (Taillandier *et al.* 2018) for studying the dynamics of CWD in mule deer in the state of California. This model addresses the ecological and epidemiological aspects of the pathogen-host-environment interface to perform spatially explicit simulations of pathogen spread (see Chapter 4.1). By simulating the potential spatiotemporal evolution of the disease through the CalCWD model, the aim of this study was to evaluate the risk of pathogen spread posed by the outbreaks in the locations where cases have been detected.

2. Materials and Methods

2.1. Study area

The state of California is located in the western United States and covers a total area of 423,955 km², making it the third largest state in the United States. Its vast size, along with the Sierra Nevada mountain range that influences marine

air circulation (WRCC 2000), gives it a diverse climate ranging from deserts in the southeast to subalpine climates in the northern and high mountain areas (Pathak *et al.* 2018). Most of the state has a Mediterranean climate, with high temperatures and low rainfall in the summer (Barbour, Keeler-Wolf & Schoenherr 2007). It is a region prone to intra- and inter-annual droughts, as well as fires in the extensive forest areas it hosts (González-Pérez *et al.* 2023).

Cervids found in California are the Roosevelt elk (*Cervus canadensis roosevelti*), the black-tailed deer (*Odocoileus hemionus columbianus*) and the mule deer (*Odocoileus hemionus hemionus*), the latter being the most abundant and potentially the most relevant to the epidemiology of CWD in the state (Otero *et al.* 2021; Schoenherr 2017). Both migratory and non-migratory populations of mule deer occur throughout most of the state (see Figure 1; Ahlborn & White 2006; Taylor 1996). Recently, CWD has been detected in mule deer in Inyo and Madera counties (Munk & Benedet 2024). The detected cases are situated 120 kilometers apart and belong to mule deer populations that do not overlap in distribution ranges, since the population in Inyo County is migratory, while the population in Madera County is not.

2.2. Model description

The CalCWD model was developed using the publicly available software GAMA (Taillandier *et al.* 2018). The complete description of the model, following the ODD (Overview, Design concepts, Details; Grimm *et al.* 2010; 2020) protocol, can be found in Chapter 4.1. A brief summary of the model description is provided here following ODD summarized structure (Grimm *et al.* 2020).

The overall purpose of CalCWD is to simulate the spatiotemporal dynamics of CWD in natural populations of mule deer in California, in order to inform policies for disease monitoring and control. To consider our model realistic

enough for its purpose, we implemented spatially explicit and stochastic processes related to mule deer ecology and CWD transmission dynamics.

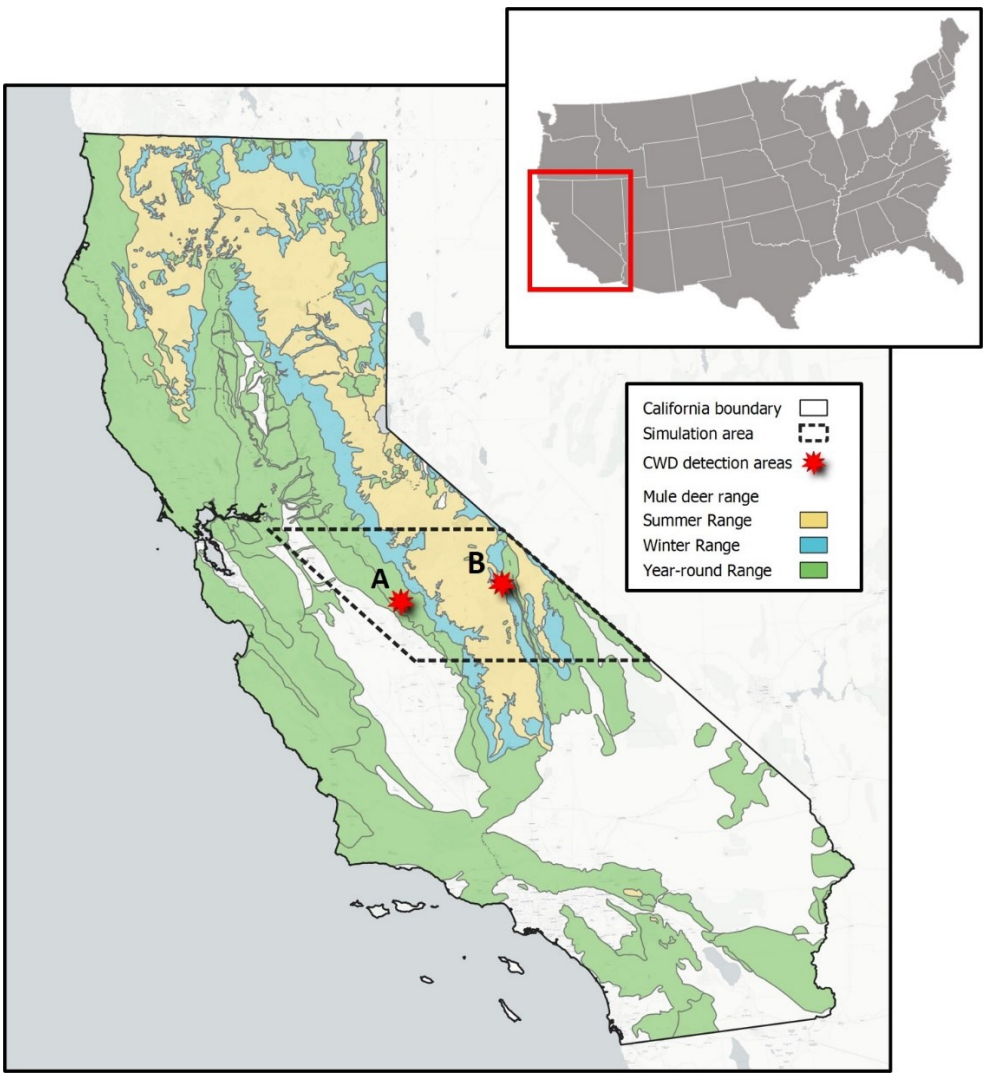

Figure 1. Location of the study area. Summer, winter, and year-round ranges of mule deer and locations where CWD cases have been detected in Madera County (A) and Inyo County (B) were provided by the CDFW. The dashed line indicates the area where the CWD dynamics simulation was conducted.

The model comprises the following entities capable of interacting with each other: mule deer, infectious carcass, and grid cell, where the latter defines the environment where the mule deer and infectious carcass agents occur. The mule deer entities include state variables related to location, age, sex, reproductive status, group membership, migratory behavior, and infection status. When a mule deer infected with CWD dies it becomes a carcass entity, which includes location and time in the environment until decomposition or scavenging as variables. The grid cell agents include variables related to mule deer habitat suitability, abundance, carrying capacity, range type (summer, winter, or year-round) and hunting pressure, as well as variables related to the presence of scavenger species and wildfire risk. As for the spatial and temporal resolution, a time step in the model represents one day and the state of California is divided into 10x10 km grid cells.

The most important processes of the model, which are computed every time step, can be divided into ecological and epidemiological related processes. Ecological can be further divided into three main categories: (1) demography, based on aging, sex-ratio, fawning, natural mortality, CWD mortality and hunting mortality; (2) social structure, which encompasses group dynamics throughout the year; and (3) movement, which includes migrations, juvenile dispersal, and other movements due to causes such as wildfires or overabundance. Additionally, intra-annual droughts are included as a potential modifier of mule deer demographic dynamics. Epidemiological processes employ an SEIR model (Susceptible, Exposed, Infectious, and Removed) which divides the pathogen's transmission into four elements: (1) within-group transmission, which is frequently-dependent (FD) transmission (Jennelle *et al.* 2014); (2) environmental transmission, which is density-dependent (DD) transmission and can have a greater impact than within-group transmission in the long-term maintenance of the pathogen (Almberg *et al.* 2021; Miller, Hobbs & Tavener 2006); (3) transmission through

visits to carcasses of infected individuals (Jennelle *et al.* 2009; Miller *et al.* 2004); and (4) a pathogen diffusion model (Garlick *et al.* 2014).

The most important design concept of the model is that the transmission of CWD depends on the demography, social dynamics, and movements of mule deer. Therefore, the spatiotemporal dynamics of the disease emerge from the evolution of the processes parameterized at the individual or cell level.

2.3. Simulations

The spatiotemporal dynamics of the CWD were simulated originating the outbreaks in the locations where it has been detected in Madera and Inyo counties (https://cdfw.maps.arcgis.com/apps/dashboards). The outbreak is initiated by the introduction of an infected adult male. Both outbreaks were simulated in conjunction with one another and separately. The simulation of outbreaks in both locations separately allows for a comparison of the risk each poses for the spread of the disease, thereby guiding the direction of management and monitoring efforts. Conversely, the simulation of outbreaks in both locations simultaneously allows for the observation of potential synergies in the disease's spread, as well as for the investigation of the potential current and future distribution of the disease in the state. For computational constraints, the spatial extent of the simulation was limited to an area of 42,000 km², which encompasses the locations of both detected cases (see Figure 1). The simulation commences on August 1st, as the model considers an initial population structure corresponding to the summer (see Chapter 4.1). The outbreak is introduced on May 1st of the following year, as the cases were detected at the beginning of this month (Munk & Benedet 2024). This allows 273 simulation steps from the start until the outbreak begins, acting as a burn-in period. The temporal extent of the simulation was defined as three years from the start of the outbreak, resulting in a total simulation duration of three years and nine months (1,368 simulation steps). The initial population was set at 625,000 mule deer for the entire state of California based on available population

estimations (CDFW 2024a), resulting in 46,160 deer in the area considered for the simulation according to the deer abundance distribution (see Chapter 4.1).

For each of the three simulations (Madera, Inyo, and both together), five iterations were conducted. From each simulation, the total number of exposed deer (i.e., those that have been infected but are not yet shedding the pathogen) was extracted for each day and cell, categorized by sex and age class, as well as the mechanism of infection (within-group, environmental, carcass, or diffusion).

2.4. Sensitivity analysis

A sensitivity analysis was conducted to assess the reliability of the results. For complex models that include numerous parameters and are computationally demanding, such as the present model, "one-step-at-a-time" (OAT) sensitivity analyses are recommended (Balesdent *et al.* 2016; Ten Broeke, Van Voorn & Ligtenberg 2016). Moreover, it is recommended to select parameters that a priori could have a greater potential impact on the results and are not based on reliable bibliographic data (Borgonovo *et al.* 2022; Saltelli *et al.* 2008). Accordingly, the parameters selected for the sensitivity analysis were the within-group transmission rate (β), the environmental transmission rate (β'), the carcass transmission rate (β_c), the diffusion rate (β_{dif}) and the probability of encountering a carcass (ρ). Furthermore, the sensitivity to the probability of fires (P_{fire}) and the probability of drought ($P_{drought}$) was analyzed, as these variables directly impact mule deer movements and demographics, thereby allowing the evaluation of the impact of these aspects on the disease dynamics (for further insight into the functioning of these parameters within the model, refer to Chapter 4.1).

First, a Morris analysis was conducted, which evaluates the net contribution of each parameter to output variability (Morris 1991). This method is a multidimensional global sensitivity analysis (the input parameters can vary simultaneously over their entire domain of definition), allowing for the

identification of nonlinear relationships between the parameters and the output and the detection of interactions between parameters (Balesdent *et al.* 2016; Likhachev 2019). In comparison to other global sensitivity analysis methods, such as Sobol analysis, Morris analysis has been proven to be effective in identifying influential parameters at a greatly reduced computational costs (Herman *et al.* 2013). This analysis involved 100 simulations sampling five different values for each parameter. However, the Morris analysis does not allow for a deeper understanding of the relationship between each parameter and the model output. Consequently, a two-dimensional "one-factor-at-a-time" (OFAT) analysis was also conducted. This is a local sensitivity analysis in which the response of the output to changes in each parameter is explored (Cariboni *et al.* 2007). This analysis involved five values for each parameter. The sensitivity analyses were conducted on a population of 10,000 mule deer in the area used for the simulation, initiating the outbreaks in both locations (Inyo and Madera counties) and with the total number of exposed individuals serving as the model output. To enhance the differentiation between the outputs obtained with the different tested values for each parameter and thus optimize the effectiveness of the sensitivity analysis, the temporal extent of the simulations was extended to 7 years after the outbreak, with a total duration of 7 years and 9 months (2,828 steps).

3. Results

3.1. Simulations

The simulations indicated that the outbreak originating in Inyo County would result in a greater number of exposures than the outbreak originating in Madera County (see Table 1). The number of exposures exhibited a gradual increase during the initial year and a half, with a notable acceleration in the second year (see Figure 2).

In the simulations that considered the Inyo County outbreak location (either alone or in conjunction with the Madera County outbreak), CWD reached the Nevada state border in an average of 2.25 years (ranging from 1 to 3 years) across 10 iterations (see Figure 3). In contrast, the pathogen spread more slowly through the simulation area when considering only the outbreak in Madera County. The CWD traveled a distance of 20 km in 3 years in the five iterations, resulting in a pathogen spread velocity of 6.7 km/year.

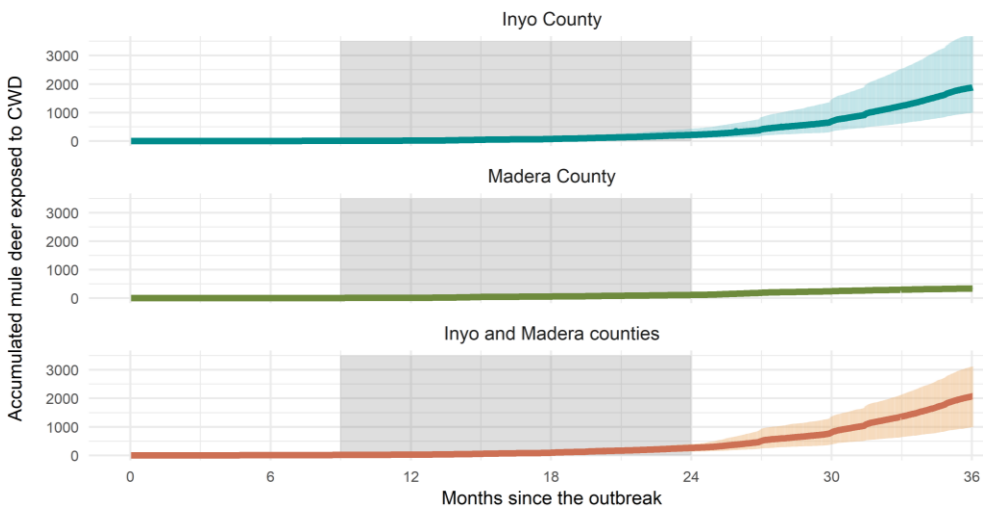

Figure 2. Number of accumulated mule deer exposed (infected but not infectious) to CWD over three years of simulations since the outbreak, considering different outbreak locations: Inyo County (upper), Madera County (middle), and both counties together (lower). The shaded area indicates the period between 1 and 2 years after the outbreak, where detection is expected to have occurred (B. Munk, personal communication).

Three years after the outbreak, at the end of the simulation, there were barely any differences in CWD prevalence rates by sex and age class, regardless of the origin of the outbreak (see Table 1). The Inyo outbreak exhibited a significantly higher prevalence than the Madera outbreak throughout the entire study area. However, prevalence rates in infected cells were higher in the Madera outbreak simulation than in the Inyo outbreak simulation, reaching rates of 40% in the cells with the highest pathogen prevalence (see Table 2).

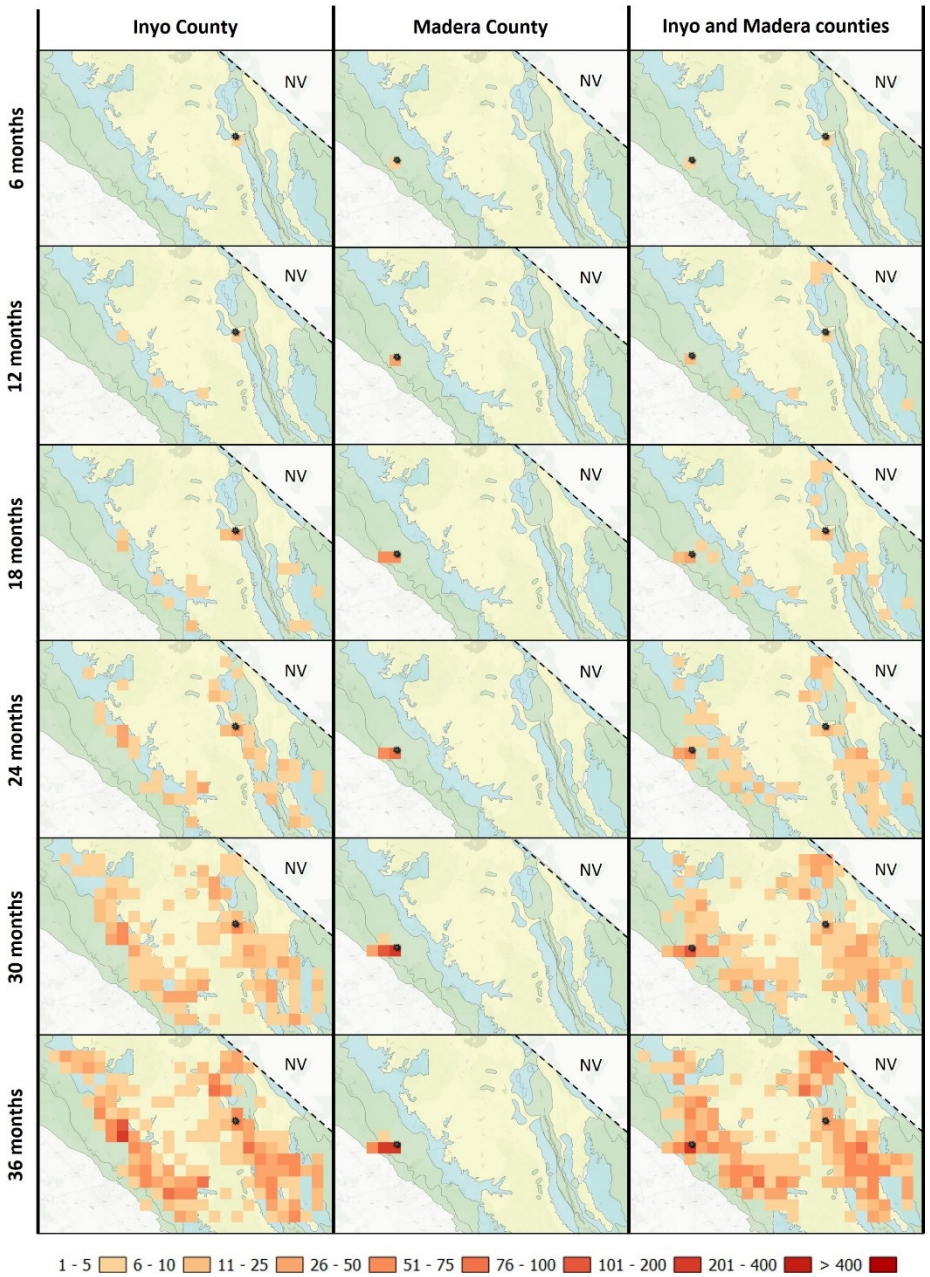

Figure 3. Number of accumulated mule deer exposed (infected but not infectious) to CWD in each cell every six-month period after the outbreak, considering different outbreak locations. The values represent the mean of five iterations for each simulation. The points represent the origin of the outbreak in each simulation, and the dashed line represents the border with the state of Nevada (NV). The shaded background areas represent the mule deer ranges: summer (yellow), winter (blue), or year-round (green).

Table 1. Accumulated number of mule deer exposed (infected but not infectious) to CWD and CWD prevalence by sex and age group in the entire simulation area at the end of the 3-year simulation. The values represent the mean and range (in parentheses) of the 5 iterations for each outbreak location. Bucks include adult and old males, while does include adult and old females.

Outbreak location	Accumulated exposed mule deer	Prevalence rates (whole simulation area)			
		Bucks	Does	Yearlings	Fawns
Inyo	1,849 (970–3,711)	3.20 % (1.83–5.94)	3.25 % (1.87–5.99)	3.19 % (1.74–6.01)	3.16 % (1.76–5.90)
Madera	337 (301–371)	0.23 % (0.14–0.29)	0.24 % (0.21–0.29)	0.23 % (0.20–0.28)	0.27 % (0.23–0.32)
Inyo and Madera	2,033 (957–3,062)	3.24 % (1.81–4.33)	3.43 % (1.75–4.59)	3.32 % (1.71–4.55)	3.39 % (1.77–4.53)

Table 2. CWD prevalence rates in mule deer in the infected cells at the end of the 3-year simulation. For each outbreak location, the mean value of the 5 iterations was calculated in each cell, and the minimum, first quartile (Q_1), median, third quartile (Q_3), and maximum of the mean values obtained for the overall infected cells are shown.

Outbreak location	Prevalence rates (infected cells)				
	Min.	Q_1	Median	Q_3	Max.
Inyo	0.09 %	2.79 %	4.17 %	5.22 %	13.73 %
Madera	0.13 %	0.34 %	10.75 %	12.90%	39.5 %
Inyo and Madera	0.07%	2.95 %	3.93 %	5.32 %	40.60 %

In terms of transmission routes, within-group and environmental transmission were the primary sources of exposure for mule deer, regardless of the origin of the outbreak (see Table 3). Diffusion, included in the model for spatial purposes, accounted for a small percentage of infections but played a key role in the spread of the pathogen in the Madera outbreak (given that the deer in this area are non-migratory, the only way for the pathogen to spread without diffusion would be through individuals' dispersal). The transmission of the pathogen by contact with infected carcasses represented a small percentage of the total number of exposures (below 1% across the total 15 iterations; see Table 3).

Table 3. Percentage of CWD exposures in mule deer caused by each transmission route at the end of the 3-year simulation for each outbreak location. The values shown represent the mean of the 5 iterations for each outbreak location, with the range indicated in parentheses.

Outbreak location	Transmission route			
	Within-group	Environmental	Infectious carcass	Diffusion model
Inyo	51.1 % (48.5–53.1)	48.3 % (46.3–50.8)	0.3 % (0.2–0.4)	0.2 % (0.1–0.4)
Madera	50.5 % (42.5–58.1)	48.6 % (41.9–56.6)	0.3% (0.0–1.0)	0.7 % (0.4–1.1)
Inyo and Madera	47.2% (40.2–53.6)	52.4 % (45.9–59.4)	0.4 % (0.3–0.7)	0.2 % (0.1–0.5)

3.2. Model evaluation

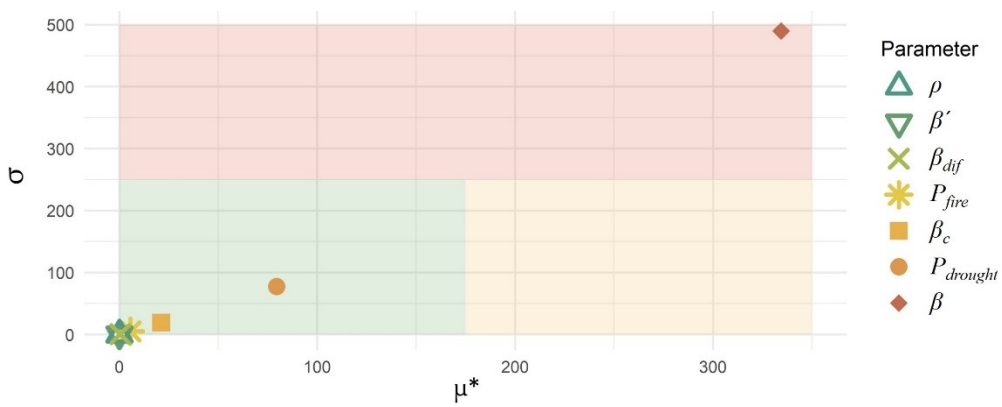

Figure 4. Absolute value of the means (μ*) and variance (σ) of the elementary effects of each factor in the Morris sensitivity analysis. The green shaded area indicates negligible effects of the parameters on the output (accumulated number of mule deer exposed in the simulation), the yellow shaded area indicates significant effects of the parameters, while the red shaded area indicates nonlinear effects or interactions between parameters (Balesdent *et al.* 2016; Campolongo, Cariboni & Saltelli 2007). The parameters included in the sensitivity analysis are the within-group transmission rate (β), the environmental transmission rate (β'), the carcass transmission rate (β_c), the diffusion rate (β_{dif}), the probability of encountering a carcass (ρ), the probability of wildfires (P_{fire}), and the probability of drought ($P_{drought}$).

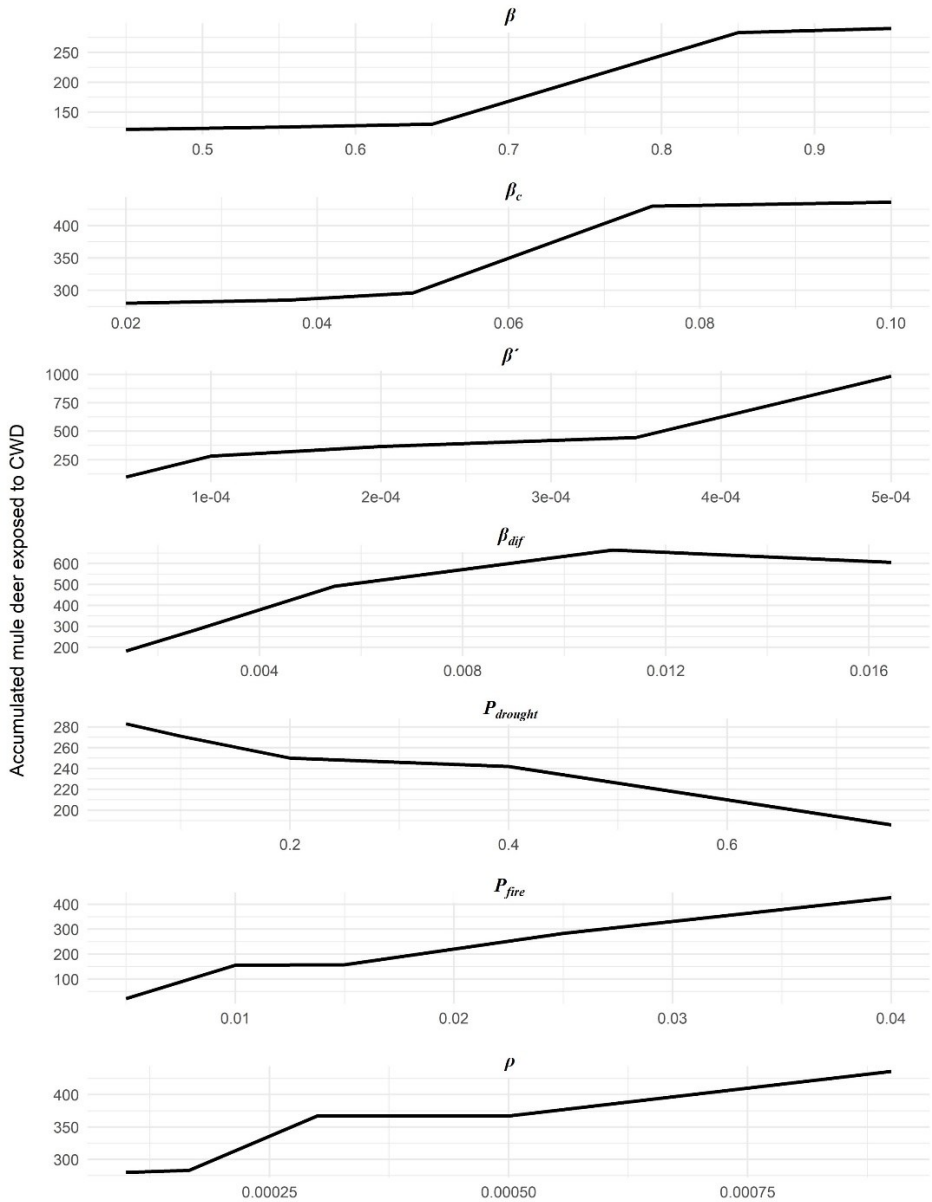

Figure 5. One-factor-at-a-time sensitivity analysis. The relationship between the output (the accumulated number of mule deer exposed to CWD at the end of the 7-year simulation following the CWD outbreak in an initial population of 10,000 mule deer) and the parameters is displayed. The following parameters were considered: within-group transmission rate (β), environmental transmission rate (β'), carcass transmission rate (β_c), diffusion rate (β_{dif}) probability of encountering a carcass (ρ), the probability of wildfires (P_{fire}) and the probability of drought ($P_{drought}$).

The impact of seven parameters (β, β', β_c β_{dif}, ρ, P_{fire}, and $P_{drought}$) on the variability of the total number of exposed mule deer at the conclusion of the simulation was assessed through a Morris sensitivity analysis. The only parameter that showed a potentially significant effect on the output was β (within-group transmission rate, see Figure 4). Nevertheless, the high variance of the β elemental effect indicates that its impact on the results is subject to a nonlinear relationship with the output or to potential interactions with other parameters included in the model. In this regard, the two-dimensional OFAT sensitivity analysis revealed that the number of exposed mule deer exhibited a positive but nonlinear relationship with the β. Furthermore, this analysis also showed positive correlation between the output and all other parameters included in the sensitivity analysis, with the sole exception of $P_{drought}$ (probability of drought), which exhibited a negative correlation (see Figure 5).

4. Discussion

The CalCWD model allows for the simulation of the dynamics of CWD in natural mule deer populations in the state of California. The model addresses comprehensively the environmental, ecological, and epidemiological components that can affect the evolution of mule deer populations and the circulation of CWD within them. Starting the outbreaks from the locations of the recently detected CWD cases in Inyo and Madera counties, the simulations provided information on the potential evolution of the disease in terms of both spatial extent and magnitude, as well as the possible current status of the disease in the state considering it may have been present in the area for some time. The simulations identified the outbreak in Inyo County as a higher risk, due to its location in a migratory population, and warned of the potential spread of the pathogen to the state of Nevada (see Table 1 and Figure 3).

The CWD outbreak in Inyo County showed a greater potential for pathogen spread within the state compared to the Madera outbreak, according to the simulations. Inyo outbreak affects a migratory population of mule deer. The movements due to migration pose a risk of spreading the pathogen to areas far from the origin of the outbreak (Altizer, Bartel & Han 2011; Farnsworth *et al.* 2006), which allowed the pathogen to reach the border with the state of Nevada, which is currently officially CWD-free (National Wildlife Health Center 2024), in an average of 2.25 years in the simulations conducted. The winter ranges of the Benton and Mono valleys, northeast of the simulation area, are highlighted as a potential entry pathway into the state of Nevada (see Figure 3). Consequently, efforts to detect CWD should be directed to these areas in order to prevent its potential spread to a yet CWD-free state.

Most exposures in the simulations that considered the Inyo County outbreak location occurred in the winter range (see Figure 3). Winter ranges are more limited than summer ranges, as snow greatly restricts mule deer distribution during the colder months, leading to greater aggregation (D'Eon & Serrouya 2005; McClure, Bissonette & Conover 2005) and potentially increasing the CWD transmission (Mysterud *et al.* 2021; Storm *et al.* 2013; Vasilyeva, Oraby & Lutscher 2015). Furthermore, from mid to late summer, prior to the breeding season, males begin to join groups of females and fawns, forming larger groups that remain until the beginning of spring (Mejia Salazar *et al.* 2016). This period spans the entire fall and winter, when migratory deer are distributed through the winter range. The formation of these larger groups may also potentially enhance CWD transmission, as infected individuals have within-group contact with a greater number of susceptible individuals (Almberg *et al.* 2011; Grear *et al.* 2010).

In contrast, the CWD outbreak simulated in Madera County affected a non-migratory mule deer population and spread more slowly. The mean spread velocity in the simulations, 6.7 km per year, is close to previously reported values (3.7 to 11 km/year in Garlick *et al.* 2014; 7.3 km/year in Xu, Merrill & Lewis

2022). Although in none of the iterations does the Madera outbreak reach the neighboring winter range of the outbreak area, this speed suggests that the pathogen could reach this winter range in 3 years (which is located 20 km away). Nevertheless, the simulation that considers both outbreak locations together suggests that this area would be affected much sooner as a consequence of the spread of the Inyo outbreak through the migratory populations. In none of the iterations in which the outbreak was initiated solely in Inyo County, did the infection reach the location of the detected case in Madera County. This suggests that both cases are independent of each other and may have different origins. If this is the case, the results indicate that Inyo County may require greater efforts for the control and monitoring of the CWD, given its higher potential for the spread of the disease. However, efforts should also be directed towards Madera County, where control appears more feasible, and a potential source of spread to other areas of the state due to human causes could be mitigated.

However, the low prevalence observed in the early phase of CWD spread represents a significant challenge for detection (Mysterud & Edmunds 2019; Winter & Escobar 2020). The simulations show no exception for California, revealing prevalences below 5% for most cells in the simulation which considers both outbreak locations (see Table 2). This raises the question of how long the pathogen may have been present in the area, considering its recent detection. The detection of CWD is improbable during the first year and likely before the third (Rees *et al.* 2012). The combination of hunting samples with other data sources, such as those from roadkill or found dead animals, can facilitate the reduction of these times (Jennelle *et al.* 2018), so the CDFW considered detecting the pathogen between 9 and 24 months after its introduction (B. Munk, personal communication). The most optimistic scenario posits a fairly contained situation of the disease, whereas the most pessimistic one suggests the possibility that the disease is quite widespread and may have even reached the border with Nevada. In this regard, efforts should be directed toward the detection of CWD on the

western slope of the Sierra Nevada at the latitude of the outbreaks. This area is identified as an expansion zone (see Figure 3). Furthermore, it would provide insights into whether both outbreaks are related and consequently how long the pathogen has been present in California.

The model includes higher interaction rates (direct transmission) and food consumption rates (environmental transmission) for bucks (adult and old males), signifying higher probability of exposure to CWD through both within-group and environmental routes in comparison to females and younger mule deer. However, differences in prevalence rates between age and sex groups are not observed as in other areas and species (Grear *et al.* 2006; Heisey *et al.* 2010b; Miller & Conner 2005; Osnas *et al.* 2009). The genetic susceptibility of each species and sex, as well as the polymorphic variants of the prion, can influence prevalence rates (Moazami-Goudarzi *et al.* 2021; Rogers, Brandell & Cross 2022), but these factors have not been considered in our model. The majority of data utilized in these studies originate from hunting (with a paucity of samples from yearlings and fawns), which could lead to biased prevalence estimations (Conner, McCarty & Miller 2000; but see Grear *et al.* 2006). Moreover, these studies focused on areas where the disease is endemic, in which environmental exposure may play a more significant role, being higher in adults due to longer exposure times and in males due to higher feeding rates (Almberg *et al.* 2011; Potapov *et al.* 2016). However, in the initial stages of disease spread, exposure may be more influenced by group dynamics, which involve larger groups in the case of females, who tend to remain with juveniles and fawns (Mejia Salazar *et al.* 2016), potentially enhancing transmission. Males may play an important epidemiological role by changing groups more frequently throughout the year (Mejia-Salazar *et al.* 2017), but similar prevalences could be expected in other age and sex classes. Consequently, control measures based on increased hunting pressure on bucks can be effective for containing the disease (Belsare *et al.* 2020b; Potapov *et al.* 2016; Uehlinger *et*

al. 2016), but measures must also be taken regarding does and young individuals to achieve disease eradication.

Whether CWD transmission is frequency-dependent (FD), density-dependent (DD), or a hybrid of both is still under debate (Winter & Escobar 2020). FD within-group transmission represents the primary mechanism of CWD transmission (Potapov *et al.* 2013; 2016; Storm *et al.* 2013). Nevertheless, DD between-group environmental transmission has been shown to play a role in pathogen persistence (Almberg *et al.* 2011; Miller, Hobbs & Tavener 2006). The CalCWD model employs a hybrid system of both mechanisms, and the results do not indicate that one mechanism is more epidemiologically relevant than the other. The diffusion model is implemented as a mechanism for between-group transmission at the cell boundaries (Xu, Merrill & Lewis 2022), and it has a low impact on the total number of exposed individuals (see Table 4). However, it has a high impact on spatial spread (as evidenced by the Madera County outbreak, which spread by diffusion; see Figure 3). Finally, although cervids can become infected through contact with infected carcasses (Jennelle *et al.* 2009; Miller *et al.* 2004), the epidemiological relevance of this transmission mechanism is uncertain, and the simulation results indicate that its epidemiological role is negligible. Consequently, control measures should focus on the hosts (Uehlinger *et al.* 2016). Carcass removal from the environment, which has been identified as a key measure for the management of African swine fever (Gervasi & Gubertì 2022), would not be expected to be effective in the case of CWD.

Forecasting the future through simulations is a challenging endeavor, as mathematically parameterizing complex natural processes necessitates making both systemic and individual assumptions that condition the results (Getz *et al.* 2018; Grimm *et al.* 2005). One illustrative example is migrations, which have a significant impact on the simulation output. While it is known that migrations can cover great distances and migratory corridors have been identified, the spatiotemporal patterns in the area remain unclear (Monteith *et al.* 2011). The

model assumes interannual variability in migrations for the same individuals (van de Kerk *et al.* 2021), as well as that migrations occur in groups (Shellard & Mayor 2020). Greater spatial consistency in migrations would result in slower pathogen spread, while group disintegration during migration would result in faster spread. In this context, the marking of mule deer individuals with GPS devices in areas where CWD cases have been detected could provide highly valuable information about the migratory patterns of these populations. This would allow the identification of potential areas for disease expansion. The validation of our model is limited by the lack of empirical data on CWD dynamics in California. However, the model is robust to variability in epidemiological parameters, with the exception of the within-group transmission rate, which has been well-studied (Almberg *et al.* 2011; Jennelle *et al.* 2014; Miller, Hobbs & Tavener 2006; Potapov *et al.* 2016; Wasserberg *et al.* 2009). Furthermore, the model is robust to variability in mule deer mobility and demography, which have been evaluated through the effects of fires, which increase mobility (van Mantgem, Keeley & Witter 2015), and droughts, which increase mortality (Jackson *et al.* 2021; Schuyler, Dugger & Jackson 2018).

The comprehensive approach of the CalCWD model, which encompasses ecological, environmental, and epidemiological aspects, offers the potential to analyze CWD dynamics in a manner that extends beyond the spatiotemporal prediction of the disease. On the one hand, the model allows for the analysis of the long-term evolution of the mule deer population in California, evaluating the potential impact of CWD on an already declining population (Loft & Bleich 2014; Webb 2013). Furthermore, the model enables the analysis of how the included parameters influence pathogen spread, thereby supporting the formulation of policy for disease management (Uehlinger *et al.* 2016). Some measures, such as an increase in hunting pressure (Belsare *et al.* 2020b; Potapov *et al.* 2016), which is already included in the model, can be tested directly. Other measures can be tested through the implementation of a complementary management module that

is under development. Therefore, the CalCWD model has the potential to inform decision-making for managing a disease that has recently entered the state. Furthermore, by modifying the input values, the model can be utilized in other locations and even for other cervid species.